Numerical simulation of stochastic two-phase flows with a DEM Method coupled to uncertainty quantification scheme

Remi Abgrall, Pietro Marco Congedo, Gianluca Geraci, Maria Giovanna Rodio

Numerical simulation of stochastic two-phase flows with a DEM Method coupled to uncertainty quantification scheme

Rémi Abgrall, Pietro Marco Congedo, Gianluca Geraci, Maria Giovanna Rodio

RESEARCH REPORT

N° 8440

December 2013

Project-Teams Bacchus

ISSN 0249-6399 ISRN INRIA/RR--8440--FR+ENG

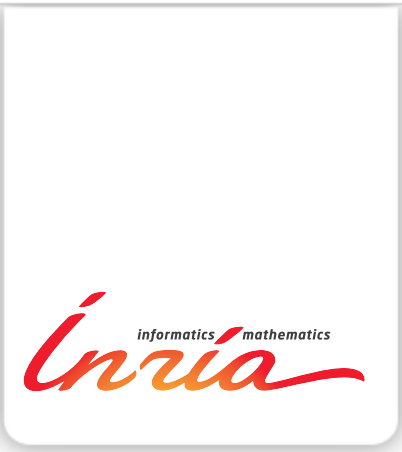

Numerical simulation of stochastic two-phase flows with a DEM Method coupled to uncertainty quantification scheme

Rémi Abgrall, Pietro Marco Congedo, Gianluca Geraci, Maria Giovanna Rodio

Project-Teams Bacchus

Research Report n° 8440 — December 2013 — 37 pages

Abstract: A new scheme for the numerical approximation of a five-equations model taking into account uncertainty quantification (UQ) is presented. In particular, the Discrete Equation Method (DEM) for the discretization of the five-equations model is modified for including a formulation based on the adaptive Semi-intrusive (aSI) scheme, thus yielding a new intrusive scheme (aSDEM) for simulating stochastic two-phase flows. Some reference test-cases are performed in order to demonstrate the convergence properties and the efficiency of the overall scheme. The propagation of initial uncertainties is evaluated in terms of mean and variance of several thermodynamic properties of the two phases.

Key-words: Uncertainty quantifications, adaptive Semi-Intrusive scheme (aSI), DEM (discrete equation method), multi-resolution, Two-phase compressible flows.

RESEARCH CENTRE
BORDEAUX – SUD-OUEST

351, Cours de la Libération
Bâtiment A 29
33405 Talence Cedex

Simulation numérique de fluides diphasiques, basée sur la méthode DEM couplée avec un schéma de quantification d'incertitude

Résumé : Un nouveau schéma est proposé pour l'approximation numérique du modèle à cinq équation en considérant la quantification d'incertitude. En particulier, le schéma DEM (Discrete Equation Method) pour la discrétisation d'un modèle cinq équations a été modifié pour le coupler avec le schéma dit 'adaptive Semi-intrusive (aSI)', en proposant ainsi un schéma intrusif pour la simulation d'un écoulement stochastique diphasique. Plusieurs cas test sont reproduits pour démontrer la convergence et l'efficacité du schéma. La propagation des incertitudes initiales est étudiée en terme de moyen et de variance de plusieurs propriétés thermodynamiques du fluide diphasique.

Mots-clés : Quantification d'incertitude, schema adaptatif semi-intrusive (aSI), DEM (discrete equation method), fluides compressible diphasiques.

Contents

1 Introduction

This work is devoted to the numerical resolution of a stochastic two-phase flow, using an adaptive semi-intrusive scheme. The context of this work is in the interface problems characterized by the coexistence of two separated phases. In some particular conditions, heat and mass transfer between the two phases can appear, increasing the complexity of observed phenomenon. The two-phase flow problems have been addressed by many authors [1, 2, 3, 4, 5, 6, 7, 8], because of their use in a large number of engineering devices. The prediction of this flow is particularly important for some specific physical problems, such as cavitation phenomena, wall corrosion, efficiency deterioration and so on.

Several studies have been focused on formulations yielding a good trade-off between physical accuracy and mathematical/numerical difficulties.

In this study, we deal with a class of methods based on compressible approach, treating the interface like a diffused zone (*i.e.* an artificial transition region where the thermodynamic conditions are unknown). This class of methods is principally affected by two important numerical issues: (i) how to define the closure laws for the average interfacial velocity and pressure and (ii) the approximation of the non-conservative terms, involving the volume fraction gradient, for shock interaction with volume fraction discontinuities.

In this field, Baer and Nunziato proposed a model [9] that was unconditionally hyperbolic and able to deal with a wide range of application. Many variants have been proposed [2, 10, 11, 12] and thanks to its ability to solve the interface problems, the model was extended to other interesting application as the evaporation fronts [13].

An original variant to Baer and Nunziato model has been proposed by Abgrall and Saurel [14]. Instead of following the most classical way, *i.e.* discretization of an averaged model, the authors developed a numerical scheme using the so-called *discrete equation method* (DEM): starting with a semi-discrete scheme for the compressible Navier-Stokes equations for each phase, a statistical average is performed in order to obtain an approximation of the mean quantities.

Anyway, the numerical complexity and implementation issues motivate the formulation of new simplified approaches. Kapila *et al.* [8] proposed a five-equations model supposing the pressure and velocity equilibrium between the phases. This model is unconditionally hyperbolic. This type of model has been used by many authors (see [1, 15, 5]) and extended to the numerical approximation of two-phase flow problem with viscous effects [16, 17].

Prediction and accuracy of these models are anyway strongly affected by the presence of numerous uncertainties. First, the models can be affected by some uncertainties, as, for example, the initial gas volume fraction (it is not possible to measure, with a good accuracy, the initial fraction during the experience) or some tuning coefficients that, for simplicity, are taken constant in the simulation (as the drag force coefficient in the drift-flux model or the heat exchange coefficient). Secondly, some uncertainties can be directly driven by the physics, geometric tolerances or experimental measurements.

Taking into account these uncertainties in the numerical simulation, is of fundamental importance for an accurate estimation of the simulation with respect to the experimental data. Anyway, this analysis is complicated by the crossing between the stochastic region (linked to the uncertainties) and shock-dominated multiphase flow.

Concerning uncertainty quantification methods, we can distinguish between non-intrusive approaches, *i.e.* where uncertainties are quantified practically by making multiple calls to a deterministic code (see the Monte Carlo family of techniques [18], the collocation family [19] and the non-intrusive Galerkin projection methods), and intrusive approaches, *i.e.* where the original deterministic code is completely modified in order to consider in the model the uncertainties and to quantify them. Concerning shock-dominated flows, the problem is to find an efficient representation of the stochastic solution, when the flow presents some discontinuities, thus producing a shock evolving in the coupled physical/stochastic space. Probabilistic uncertainty quantification (UQ) approaches represent the inputs as random variables and seek to construct a statistical characterization of few quantities of interest.

Wan and Karniadakis have introduced an adaptive class of methods for solving the discontinuity issues by using local basis functions, the multi-element generalized Polynomial Chaos (ME-gPC), see [20]. This strategy deals with an adaptive decomposition of the domain on which local basis are employed. In order to treat discontinuous response surfaces, [21, 22] applied a multiresolution analysis to Galerkin projection schemes. The intrusive Galerkin approach may lead to optimal representation of the solution, exhibiting an exponential convergence, if a proper basis is chosen. However the intrusive Galerkin approach results in a larger system of equations than in deterministic case with, in addition, a different structure that requires a new class of solver and numerical code. Despite this issue, the intrusive Galerkin approach can be demonstrated to have substantial advantages with respect non-intrusive approach, not only for idealized systems, but also for large-scale applications [21]. Advancements have

been achieved in the Galerkin intrusive scheme where the wavelets formulation has been introduced in order to modify the basis of approximation [23]. It modifies the basis, by enriching the space with a hierarchical structure according to the regularity of the solution. However the Galerkin approach presented in [23] remains very problem-dependent. In fact, using a Roe-type solver requires to know the eigenstructure of the Roe matrix explicitly; this can be very complex. More over, *ad hoc* entropy fix should be adopted, thus increasing the numerical cost associated to the representation of discontinuous solution [24]. This original approach has been further improved to obtain a more efficient scheme employing a multiresolution adaptive strategy [23]. However actually this approach is limited by the spatial and time discretization accuracy that could dominate the overall accuracy of the global scheme. In [25], an intrusive formulation of the stochastic Euler equations based on Roe variables is presented. It is shown that the Roe variable formulation is robust for supersonic problems where the conservative variable formulation fails, but only for localized basis functions of the generalized chaos representation. For global Legendre polynomials, the discontinuities in stochastic space lead to oscillations and unphysical behavior of the solution and numerical instability. Wavelet functions are more robust in this respect, and do not yield oscillations around discontinuities in stochastic space, but need very regular grids.

More recently, in the context of uncertainty quantification studies, Abgrall and Congedo [26] proposed a novel semi-intrusive approach that extend in a straightforward and natural way, the representation of the variables in the physical space also along the stochastic space. This approach leads to a very flexible scheme able to handle whatever form of probability density function even time varying and discontinuous. One of the prominent advantage of this kind of approach is the possibility to extend in an easier way an existing deterministic code to its stochastic counterparts.

Recently, a cell-average setting multiresolution framework has been coupled with the SI scheme. Some reference test-cases are performed to demonstrate the convergence properties and the efficiency of the overall scheme: the linear advection problem for both smooth and discontinuous initial conditions, the inviscid Burgers equation and the 1D Euler system of equations to model an uncertain shock tube problem obtained by the well-known Sod shock problem [27].

Actually, for the stochastic investigation in a two-phase flow, the non-intrusive approach has been, clearly, favored, but the number of contributions is actually low [28, 29, 30, 31, 32, 33]. However, the non-intrusive method result in a expensive computational cost, compared to intrusive method. To our knowledge, in literature there is only one contribution about an intrusive method applied to a two-phase flow investigation proposed by Petterson et al. [34]. They proposed a five equations model (one pressure and one velocity) coupled to a perfect gas equation of state for both the phases. The source term in the transport equation for the volume fraction α, is taken equal to zero (they neglect $K\nabla(u)$ - see system (7)), so they impose the gas volume fraction not to vary across acoustic waves. At this point, the model is no longer a mixture model, but is valid only for interface problems (see [16]). Then, in order to obtain the stochastic formulation of the two-phase problem, they modified the fluxes, including the stochastic variable.

In this study, a new scheme for the numerical approximation of a five-

equation model based on the DEM method using an adaptive semi-intrusive scheme for the uncertainty quantification is presented. On the contrary of [34], we consider a general formulation, solving the whole system (7). The numerical issues determined by solving the term $K\nabla(u)$, are solved using the DEM approach. The avantages to use this scheme are explained in section 3, but, for more details, Refs. [17, 5] are strongly recommended.

In particular, the MR framework with real-time adaptivity in the stochastic space, is adapted and coupled with the DEM scheme for the discretization of one dimensional two-phase five-equations model [14].

This paper is organized as follows. In section 2, at first, a description of the five equation model and of the semi-discrete equation obtained with the DEM method is explained. The thermodynamic closure is addressed in section 2.2. Then, in Section 4.3, main elements of the adaptive-semi-intrusive scheme, applied to the DEM model, (aSDEM) are presented. Both the original semi-intrusive scheme and its adaptive version are also presented in sections 4.1 and 4.2 respectively. In section 5, three test-cases are considered for the assessment of the proposed formulation. Final remarks follows in section 6.

2 Mathematical model

The aim of the paper is to develop an overall numerical scheme to propagate uncertainties in the DEM solver. Let consider a generic governing equation for $u(x,t,\xi)$

$$\mathcal{L}(x,t,\xi;u(x,t,\xi)) = \mathcal{S}(x,t,\xi) \tag{1}$$

where $x \in \Omega$ is the physical coordinate, $t \in T$ the time coordinate and $\xi \in \Xi$ the stochastic coordinate and $\mathcal{L}$ is a differential/algebraic operator and $\mathcal{S}$ a source term, both defined on the domain $\Omega \times T \times \Xi$. The operator $\mathcal{L}$ can involve differentiations in space and time and can be non linear. Obviously mathematical well-posed problems are obtained imposing proper boundary and initial conditions. The aim of the UQ analysis is to obtain a statistic characterization of the unknown u (or eventually other variable of interest referred in the following as output). Depending from the scope of the analysis the statistical outcomes could be different: statistical moments, probability distributions *etc.*

In all the numerical test cases presented in this work, except for those concerning explicitly the high-order moments, the quantities of interest, systematically computed on the output u, have been the expectancy $\mathbb{E}(u,x,t)$ and the second central moments, *i.e.* the variance $\mathrm{Var}(u,x,t)$ following the definitions

$$\begin{aligned} \mathbb{E}(u,x,t) &= \int_\Xi u(x,t,\xi)p(\xi,t)\mathrm{d}\xi \\ \mathrm{Var}(u,x,t) &= \int_\Xi \left(u(x,t,\xi) - \mathbb{E}(u)\right)^2 p(\xi,t)\mathrm{d}\xi. \end{aligned} \tag{2}$$

The stochastic parameter is supposed to have a distribution over the space Ξ. This distribution is considered uniform in this work, without loss of generality of the approach as already demonstrated in [26, 35]. The proposed method belongs to the so-called *intrusive* class of method for the UQ. Therefore the propagation of the uncertainties is not performed by a recursive call of an existing numerical code, but a novel numerical scheme need to be formulated. In

particular the method here proposed can be defined semi-intrusive, following Abgrall and Congedo [26], being the theoretical framework closely related to the deterministic counterpart. The number of equation to solve is preserved and there is no need to modify the flux functions as, for instance, mandatory for the intrusive Polynomial Chaos class of methods. For further details on the advantages of a such a kind of approach the reader can refer to [26, 36].

In this section, we illustrate the coupling of the two-phase flows resolution scheme with the adaptive multiresolution semi-intrusive scheme. The two-phase model is based on a five-equation model with a single pressure and a single velocity. It is obtained imposing the asymptotic reduction of a seven equation model and it is discretized with a DEM approach, following Abgrall [5]. We recall briefly the governing equations and the principles of the DEM approach, since it has already been extensively explained in [5, 14, 37].

2.1 The five equations model

The well-known Baer & Nunziato [9] model is composed by the conservative equations of each phase and one transport equation for each volume fraction of phases (in this case no heat and mass transfer is considered):

$$
\left\{
\begin{array}{lcll}
\dfrac{\partial \alpha_1}{\partial t} & = & -\mathbf{u}_I \cdot \nabla \alpha_1 & +\mu(p_1 - p_2) \\
\dfrac{\partial \alpha_1 \rho_1}{\partial t} + \nabla(\alpha_1 \rho_1 \mathbf{u}_1) & = & 0 & \\
\dfrac{\partial \alpha_1 \rho_1 \mathbf{u}_1}{\partial t} + \nabla(\alpha_1 \rho_1 \mathbf{u}_1 \otimes \mathbf{u}_1) + \nabla(\alpha_1 p_1) & = & p_I \nabla(\alpha_1) & +\lambda(\mathbf{u}_2 - \mathbf{u}_1) \\
\dfrac{\partial \alpha_1 \rho_1 E_1}{\partial t} + \nabla(\alpha_1(\rho_1 E_1 + p_1)\mathbf{u}_1) & = & p_I \mathbf{u}_I \cdot \nabla(\alpha_1) & +\lambda \mathbf{u}_I \cdot (\mathbf{u}_2 - \mathbf{u}_1) + \\
 & & & -\mu p_I (p_1 - p_2) \\
\dfrac{\partial \alpha_2}{\partial t} + \mathbf{u}_I \cdot \nabla \alpha_2 & = & & -\mu(p_1 - p_2) \\
\dfrac{\partial \alpha_2 \rho_2}{\partial t} + \nabla(\alpha_2 \rho_2 \mathbf{u}_2) & = & 0 & \\
\dfrac{\partial \alpha_2 \rho_2 \mathbf{u}_2}{\partial t} + \nabla(\alpha_2 \rho_2 \mathbf{u}_2 \otimes \mathbf{u}_2) + \nabla(\alpha_2 p_2) & = & p_I \nabla(\alpha_2) & -\lambda(\mathbf{u}_2 - \mathbf{u}_1) \\
\dfrac{\partial \alpha_2 \rho_2 E_2}{\partial t} + \nabla(\alpha_2(\rho_2 E_2 + p_2)\mathbf{u}_2) & = & p_I \mathbf{u}_I \cdot \nabla(\alpha_2) & -\lambda \mathbf{u}_I \cdot (\mathbf{u}_2 - \mathbf{u}_1) + \\
 & & \underbrace{\qquad\qquad}_{Non\ conservative\ terms} & \underbrace{+\mu p_I (p_1 - p_2)}_{Relaxation\ terms}
\end{array}
\right. \tag{3}
$$

where the subscripts 1 and 2 refer to the two phases k. Quantities α_k, ρ_k, $\mathbf{u}_k$, p_k, E_k are the volume fraction, the density, the velocity vector, the pressure and the total energy, respectively for each phase k. The last one is defined as $E_k = e_k + 0.5u_k^2$. The interface velocity and the pressure are indicated with u_I and p_I, respectively. These ones are defined in [9] as $u_I = u_2$ and $p_I = p_1$, with 1 and 2 corresponding to the gas and the liquid phases, respectively. Other possible definitions of interface variables are given in [14, 4].

Parameters λ and μ represent the dynamic compaction viscosity and the relaxation velocity parameter, respectively.

The system (3) can be expressed in vectorial form as follows:

$$\frac{\partial U}{\partial t} + \frac{\partial}{\partial x} F(U) + B(U)\frac{\partial \alpha_1}{\partial x} = S(U) \tag{4}$$

or, after some manipulation:

$$\frac{\partial U}{\partial t} + FT(U) = S(U) \tag{5}$$

where

$$U = \begin{pmatrix} \alpha_1 \\ \alpha_1\rho_1 \\ \alpha_1\rho_1\mathbf{u}_1 \\ \alpha_1\rho_1 E_1 \\ \alpha_2 \\ \alpha_2\rho_2 \\ \alpha_2\rho_2\mathbf{u}_2 \\ \alpha_2\rho_2 E_2 \end{pmatrix}, \qquad FT(U) = \frac{\partial}{\partial x} F(U) + B(U)\frac{\partial \alpha_1}{\partial x},$$

$$F(U) = \begin{pmatrix} 0 \\ \alpha_1\rho_1\mathbf{u}_1 \\ \alpha_1(\rho_1\mathbf{u}_1 \otimes \mathbf{u}_1) + p_1 \\ \alpha_1(\rho_1 E_1 + p_1)\mathbf{u}_1 \\ 0 \\ \alpha_2\rho_2\mathbf{u}_2 \\ \alpha_2(\rho_2\mathbf{u}_2 \otimes \mathbf{u}_2) + p_2 \\ \alpha_2(\rho_2 E_2 + p_2)\mathbf{u}_2) \end{pmatrix}$$

$$B(U) = \begin{pmatrix} \mathbf{u}_I \\ 0 \\ -p_I \\ -p_I\mathbf{u}_I \\ \mathbf{u}_I \\ 0 \\ -p_I \\ -p_I\mathbf{u}_I \end{pmatrix}, \quad S(U) = \begin{pmatrix} \mu(p_1 - p_2) \\ 0 \\ \lambda(\mathbf{u}_2 - \mathbf{u}_1) \\ \lambda\mathbf{u}_I \cdot (\mathbf{u}_2 - \mathbf{u}_1) - \mu p_I(p_1 - p_2) \\ -\mu(p_1 - p_2) \\ 0 \\ -\lambda(\mathbf{u}_2 - \mathbf{u}_1) \\ -\lambda\mathbf{u}_I \cdot (\mathbf{u}_2 - \mathbf{u}_1) + \mu p_I(p_1 - p_2) \end{pmatrix}.$$

Supposing the mechanical equilibrium, the equality of pressure and velocity can be obtained in the limit of a stiff mechanical relaxation as in [8, 1], *i.e.* the relaxation parameters, λ and μ are taken as infinite:

$$\mu = \frac{1}{\epsilon}, \qquad \lambda = \frac{1}{\epsilon}, \quad where \quad \epsilon \to 0^+. \tag{6}$$

As a consequence, the asymptotic development allows to find the solution such that the relaxation terms go to zero (for more details concerning asymptotic development, Refs. [1, 5, 17] are strongly recommended). Then, after some

algebraic manipulations of system (3), the reduced model is thus obtained:

$$\begin{cases} \dfrac{\partial \alpha_1}{\partial t} + \mathbf{u}\cdot\nabla\alpha_1 = \dfrac{\rho_2 c_2^2 - \rho_1 c_1^2}{\frac{\rho_1 c_1^2}{\alpha-1} + \frac{\rho_2 c_2^2}{\alpha_2}}\nabla\mathbf{u} = K\cdot\nabla(u) \\ \dfrac{\partial \alpha_1\rho_1}{\partial t} + \nabla(\alpha_1\rho_1\mathbf{u}) = 0 \\ \dfrac{\partial \alpha_2\rho_2}{\partial t} + \nabla(\alpha_2\rho_2\mathbf{u}) = 0 \\ \dfrac{\partial \rho\mathbf{u}}{\partial t} + \nabla(\rho_k\mathbf{u}\otimes\mathbf{u} + p) = 0 \\ \dfrac{\partial E}{\partial t} + \nabla((E+p)\mathbf{u}) = 0 \end{cases} \tag{7}$$

where $\rho = \alpha_1\rho_1 + \alpha_2\rho_2$, $E = \alpha_1\rho_1 e_1 + \alpha_2\rho_2 e_2$, p and $\mathbf{u}$ are the mixture density, mixture total energy, the mixture pressure and the mixture velocity, respectively. Finally, c_k is the sound of speed of each phase.

We remember that $\alpha_1 + \alpha_2 = 1$, so only a single phase is considered in the unknowns of the system that, for the system 7 are: α_1, ρ_1, ρ_2, e_1, e_2, p and u. There are seven unknowns. Then, in order to close the system (7), an equation of state (EOS) for each pure phase is demanded in order to define all the thermodynamic properties. This model involves mechanical equilibrium between the phases at any time, as it is evident looking at the presence of only one pressure p and only one velocity vector, $\mathbf{u}$, in the system 7. Finally, the computations presented in this work rely on the five-equation model.

2.2 Thermodynamic Closure

Defining thermodynamic properties is necessary in order to close the system describing compressible flows. Here, we consider as the equation of state (EOS), the Stiffened Gas (SG) to describe both liquid and gas phases:

$$\rho_k e_k = \frac{(p_k + \gamma p_{k,\infty})}{\gamma_k - 1} \tag{8}$$

where e_k is the phase internal energy, p_k is the phase pressure, γ_k and $p_{k,\infty}$ are two constants characterizing each fluid. The constants for these fluids are provided in table 2. The mixture SG-EOS can be easily obtained using the EOS of the single phases, by applying the definition of the total mixture energy equation:

$$\rho E = \alpha_1\rho_1 e_1 + \alpha_2\rho_2 e_2. \tag{9}$$

The internal energy of each phase, e_k, can be replaced by the Eq.(8), obtaining the mixture total energy as a function of the phase pressure. Under pressure equilibrium, we obtain the following expression for the pressure mixture:

$$p(\rho, e, \alpha_k) = \frac{\rho(E - \frac{\alpha_1\rho_1 q_1}{\rho} - \frac{\alpha_2\rho_2 q_2}{\rho}) - \left(\frac{\alpha_1\gamma_1 p_{\infty,1}}{\gamma_1 - 1} + \frac{\alpha_2\gamma_2 p_{\infty,2}}{\gamma_2 - 1}\right)}{\frac{\alpha_1}{\gamma_1 - 1} + \frac{\alpha_2}{\gamma_2 - 1}} \tag{10}$$

In this paper, the term q is supposed equal to zero for each phase.

3 The numerical scheme

The DEM approach has been derived in [14] and in [5] for the five-equations model. We recall here the main lines of the scheme.

First, we remember that the DEM consists in applying at a discrete level, the same procedure used to obtain a compressible multiphase model, *i.e.*:

1. Suppose that each pure fluid is governed by the Euler equations.

2. Introduce, for each phase, the characteristic function X_k that satisfies the topological equation:

$$\frac{\partial X_k}{\partial t} + \sigma \cdot \nabla X_k = 0, \;\; with \;\; X_k = \begin{cases} 1 & \text{if } (\vec{x},\text{t}) \text{ belongs to phase k} \\ 0 & \text{otherwise} \end{cases} \tag{11}$$

   where σ is the interface velocity between the two phases.

3. An averaging procedure, $\mathcal{E}(\cdot)$, as in Drew and Passmann [38], is applied to the Euler equations (see [14]).

4. A statistical average is performed in order to obtain an approximation of the mean quantities.

Obtaining the semi-discrete numerical approximation of the two-phase system (7) demands a two-steps procedure. First, the DEM method, previously described, is applied to a seven equations model, *i.e.* to the system (3). After obtaining its semi-discrete numerical approximation, a relaxation procedure is applied, always at a discrete level, in order to reach a mechanical equilibrium.

Now, let us suppose that at time t, the computational domain Ω is divided into the cells $\mathcal{C}_i =]x_{i-1/2}, x_{i+1/2}[$. At a time $t = t + s$ (with s small), we assume that the interface in $x_{i+1/2}$ moves at a velocity $\sigma_{i+1/2}$ and the interface in $x_{i-1/2}$ moves at a velocity $\sigma_{i-1/2}$. As a consequence, the cell $\mathcal{C}_i$ evolves in $\bar{\mathcal{C}}_i =]x_{i-1/2} + s\sigma_{i-1/2}, x_{i+1/2} + s\sigma_{i+1/2}[$ (see figure 1). The cell may be either smaller or larger than the original ones $\mathcal{C}_i$, depending on the signs of the velocities. Then, we denote with $F(U_L, U_R)$ the Godunov numerical flux

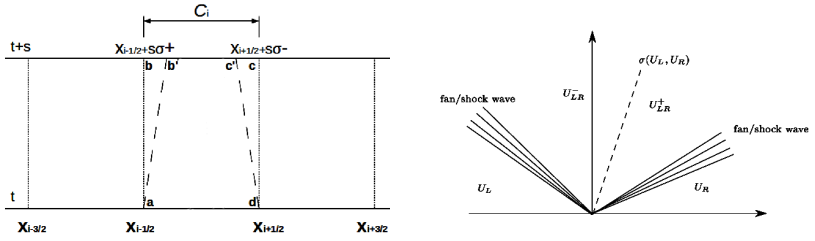

(a) (b)

Figure 1: (a) Subdivision of computational domain. (b) The various states in the Riemann problem between states U_L and U_R.

between the states U_L and U_R, and with $F^{lag}(U_L, U_R)$ the flux across the contact

discontinuity between the states U_L and U_R (see figure 1). The relation between the two fluxes is equal to :

$$F^{lag}(U_L,U_R) = F(U_{LR}^+) - \sigma(U_L,U_R)U_{LR}^+ = F(U_{LR}^-) - \sigma(U_L,U_R)U_{LR}^-, \quad (12)$$

where the superscripts $\pm$ denote the state on the right and on the left of the contact discontinuity as in figure 1.

The semi-discrete scheme for the reduced five equations model in 1D is:

$$\left\{\begin{array}{l} \dfrac{\partial \alpha_1}{\partial t} = FT(U_1) + \dfrac{\alpha_1\alpha_2}{\alpha_2\rho_1a_1^2+\alpha_1\rho_2a_2^2}\left\{\dfrac{FT(U_8)}{\alpha_2\rho_2\chi_2} - \dfrac{u_2FT(U_7)}{\alpha_2\rho_2\chi_2} + \dfrac{\frac{{u_2}^2}{2} - e_2 - \rho_2\kappa_2}{\alpha_2\rho_2\chi_2}FT(U_6) + \right. \\ \qquad \left. + \dfrac{\rho_2^2\kappa_2FT(U_1)}{\alpha_2\rho_2\chi_2} - \dfrac{FT(U_4)}{\alpha_1\rho_1\chi_1} + \dfrac{u_1FT(U_3)}{\alpha_1\rho_1\chi_1} - \dfrac{\frac{{u_1}^2}{2} - e_1 - \rho_1\kappa_1}{\alpha_1\rho_1\chi_1}FT(U_2) - \dfrac{\rho_1^2\kappa_1FT(U_5)}{\alpha_1\rho_1\chi_1}\right\} \\ \dfrac{\partial \alpha_1\rho_1}{\partial t} = FT(U_2) \\ \dfrac{\partial \alpha_2\rho_2}{\partial t} = FT(U_6) \\ \dfrac{\partial \rho u}{\partial t} = FT(U_3) + FT(U_7) \\ \dfrac{\partial \rho E}{\partial t} = FT(U_4) + FT(U_8) \end{array}\right. \quad (13)$$

where χ_k and κ_k, are defined as follows:

$$\chi_k = \left(\frac{\partial e_k}{\partial P_k}\right)_{\rho_k} \;;\; \kappa_k = \left(\frac{\partial e_k}{\partial \rho_k}\right)_{p_k} \quad (14)$$

where e_k is the phase internal energy.

As explained before, the vector $FT(U_j)$, with $j = 1, ..., 8$, is the sum of two contributions, *i.e.* the flux of hyperbolic system (conservative term) and the non-conservative terms, obtained for each equation of the system (3).

The correspondence of the semi-discrete system (13) with the model (7) has been demonstrated in [5]. Note that this method features initially two different thermodynamic states of phases, attaining, finally, a mechanical equilibrium. On the contrary, a direct discretization of the system (7) means directly the equality of initial pressure and velocity of the phases.

Following the adaptive multiresolution semi-intrusive scheme step is, now, to define the vector $FT(U_j)$ that for each component is composed by a conservative and a non-conservative terms:

$$\begin{aligned} FT(U_j) = &\frac{1}{\triangle x}\,\mathcal{E}\left(X(x_{i+1/2},t)F(U_{i+1/2}^*) - X(x_{i-1/2},t)F(U_{i-1/2}^*)\right) + \\ &+\frac{1}{\triangle x}\left(\mathcal{E}([X]_{j=0})F^{lag}(U_i^-,U_{i-1}^+) - \mathcal{E}([X]_{j=N})F^{lag}(U_i^+,U_{i+1}^-)\right), \end{aligned} \quad (15)$$

where $U_{i+1/2}^*$ (or $U_{i+1/2}^*$) denotes the solution of Riemann problem between U_i^+ and U_{i+1}^- (respectively,U_{i-1}^+ and U_i^-). Quantities $[X]_{j=0}$ and $[X]_{j=N}$ are the jump of X at the beginning and at the end of computational cell, respectively.

Following the procedure demonstrated in [14, 5], the idea of DEM method is to avoid the introduction of approximated estimation of fluxes expectancy. This is estimated basing on the probability to find in two neighbor cells the

same phase or two different phases (see the "flow patterns" in the table 1). As a consequence, we can define the flux indicator as in the following:

$$\beta^{(l,r)}_{i+1/2} = sign(\sigma(U^l_i, U^r_{i+1})) = \begin{cases} 1 & if\ \sigma(U^l_i, U^r_{i+1}) \geq 0, \\ -1 & if\ \sigma(U^l_i, U^r_{i+1}) < 0, \end{cases}$$

where l and r indicate the phase at the left and the right of interface, respectively. Then, conservative and non-conservative terms of (15) can be developed supposing the four instances. Again, for sake of clarity, we briefly recall the main ideas of this strategy [14, 5].

Flow Patterns	Jump indicator	Flux Indicator
$\Sigma_1 - \Sigma_2$	$[X]_{1,1} = 0$	$\left(\beta^{(1,2)}_{i+1/2}\right)$
$\Sigma_1 - \Sigma_1$	$[X]_{1,2} = \begin{cases} -1\ if\ \sigma(1,2) > 0 \\ 0 \quad otherwise \end{cases}$	1
$\Sigma_2 - \Sigma_1$	$[X]_{2,1} = \begin{cases} 1\ if\ \sigma(2,1) > 0 \\ 0 \quad otherwise \end{cases}$	$\left(\beta^{(2,1)}_{i+1/2}\right)$
$\Sigma_2 - \Sigma_2$	$[X]_{2,2} = 0$	0

Table 1: The various flow configurations at cell boundary $i + 1/2$.

The terms of the vector $FT(U_j)$ (see (15)) can be defined as:

$$\mathcal{E}\left(X(x_{i+\frac{1}{2}}, t)F(U^*_{i+\frac{1}{2}})\right) = \mathcal{P}_{i+\frac{1}{2}}(\Sigma_1 - \Sigma_1)F(U^{(1)}_i, U^{(1)}_{i+1}) + \\ + \mathcal{P}_{i+\frac{1}{2}}(\Sigma_1 - \Sigma_2)\left(\beta^{(1,2)}_{i+\frac{1}{2}}\right)F(U^{(1)}_i, U^{(2)}_{i+1}) + \mathcal{P}_{i+\frac{1}{2}}(\Sigma_2 - \Sigma_1)\left(\beta^{(2,1)}_{i+\frac{1}{2}}\right)F(U^{(2)}_i, U^{(1)}_{i+1})$$

$$\mathcal{E}\left(X(x_{i-\frac{1}{2}}, t)F(U^*_{i-\frac{1}{2}})\right) = \mathcal{P}_{i-\frac{1}{2}}(\Sigma_1 - \Sigma_1)F(U^{(1)}_{i-1}, U^{(1)}_i) + \\ + \mathcal{P}_{i-\frac{1}{2}}(\Sigma_1 - \Sigma_2)\left(\beta^{(1,2)}_{i-\frac{1}{2}}\right)F(U^{(1)}_{i-1}, U^{(2)}_i) + \mathcal{P}_{i-\frac{1}{2}}(\Sigma_2 - \Sigma_1)\left(\beta^{(2,1)}_{i-\frac{1}{2}}\right)F(U^{(2)}_{i-1}, U^{(1)}_i)$$

$$\mathcal{E}\left([X]_N F^{lag}(U^{N(w)}_i, U^-_{i+1})\right) = \mathcal{P}_{1+1/2}(\Sigma_1, \Sigma_2)\left(\beta^{(1,2)}_{i+1/2}\right)F^{lag}(U^{(1)}_i, U^{(2)}_{i+1}) + \\ - \mathcal{P}_{1+1/2}(\Sigma_2, \Sigma_1)\left(\beta^{(2,1)}_{i+1/2}\right)F^{lag}(U^{(2)}_i, U^{(1)}_{i+1})$$

$$\mathcal{E}\left([X]_0 F^{lag}(U^+_{i-1}, U^0_i)\right) = -\mathcal{P}_{1-1/2}(\Sigma_1, \Sigma_2)\left(\beta^{(1,2)}_{i-1/2}\right)F^{lag}(U^{(1)}_{i-1}, U^{(2)}_i) + \\ + \mathcal{P}_{1-1/2}(\Sigma_2, \Sigma_1)\left(\beta^{(2,1)}_{i+1/2}\right)F^{lag}(U^{(2)}_{i-1}, U^{(1)}_i)$$

It remains to evaluate the term of probability, $\mathcal{P}_{i\pm1/2}(\Sigma_p, \Sigma_q)$ (see [14]). For simplicity, we show the final formulation for $i + 1/2$:

$$\mathcal{P}_{i+1/2}(\Sigma_1, \Sigma_1) = \min\left(\alpha^{(1)}_i,\ \alpha^{(1)}_{i+1}\right)\mathcal{P}_{i+1/2}(\Sigma_1, \Sigma_2) = \max\left(\alpha^{(1)}_i - \alpha^{(1)}_{i+1}, 0\right)\mathcal{P}_{i+1/2}(\Sigma_2, \Sigma_1) = \max\left(\alpha^{(2)}_i -$$

where Σ_k indicates the phase, with $k = 1, 2$.

The system (13) can be written in vectorial form as follows:

$$\frac{W_i^{n+1} - W_i^n}{\Delta t} + \frac{\Delta F(W)_i}{\Delta x} = 0 \tag{17}$$

where

$$W = \begin{pmatrix} \alpha_1 \\ \alpha_1\rho_1 \\ \alpha_2\rho_2 \\ \rho\mathbf{u} \\ \rho E \end{pmatrix} \tag{18}$$

is the conservative variables vector of the reduced five equations model and

$$\Delta F(W) = \Delta x \begin{pmatrix} FT(U_1) + \frac{\alpha_1\alpha_2}{\alpha_2\rho_1 a_1^2 + \alpha_1\rho_2 a_2^2}\left\{ \frac{FT(U_8)}{\alpha_2\rho_2\chi_2} - \frac{u_2 FT(U_7)}{\alpha_2\rho_2\chi_2} + \frac{\frac{{u_2}^2}{2} - \varepsilon_2 - \rho_2\kappa_2}{\alpha_2\rho_2\chi_2} FT(U_6) + \frac{\rho_2^2\kappa_2 FT(U_1)}{\alpha_2\rho_2\chi_2} + \right. \\ \left. - \frac{FT(U_4)}{\alpha_1\rho_1\chi_1} + \frac{u_1 FT(U_3)}{\alpha_1\rho_1\chi_1} - \frac{\frac{{u_1}^2}{2} - \varepsilon_1 - \rho_1\kappa_1}{\alpha_1\rho_1\chi_1} FT(U_2) - \frac{\rho_1^2\kappa_1 FT(U_5)}{\alpha_1\rho_1\chi_1} \right\} \\ FT(U_2) \\ FT(U_6) \\ FT(U_3) + FT(U_7) \\ FT(U_4) + FT(U_8) \end{pmatrix}.$$

The numerical flux F(U) is obtained thanks to an approximate Riemann solver. It defines the contact speed $\sigma(U_L, U_R)$, allowing to define the Lagrangian flux F^{lag} (see equation (12)). The Riemann problems solution is sought for times that satisfy a CFL conditions of the type:

$$|\lambda_{max}| \frac{\Delta x}{\Delta t} \leqslant \frac{1}{2}.$$

In this paper, we have used the relaxation solver [39] for all computations (see [5] for more details).

3.1 Predictor-corrector DEM solver

Now, we extend the approximation of the scheme (17) to a second order following an extension of a MUSCL approach. This approach for a multiphase flow had been proposed in [14] and in this study we apply exactly the same extension. Anyway we recall here the main lines.

The following scheme is an extension of a predictor-corrector scheme for a general conservation law $\partial U/\partial t + \partial F/\partial x$=0 (see [40]). We assume an uniform mesh Δx and we define four steps :

Step 1: From U_j^n, compute the limited slope δU and evaluate:

$$U_{i-\frac{1}{2}}^n = U_i^n - \frac{\Delta x}{2}\delta U_i^n \quad \text{and} \quad U_{i+\frac{1}{2}}^n = U_i^n + \frac{\Delta x}{2}\delta U_i^n$$

.

Step 2: Evaluate the solution over half a time step:

$$U_i^{n+\frac{1}{2}} = U_i^n - \frac{\Delta t}{2\Delta x}\left(F(U_{i+\frac{1}{2},l}^n, U_{i+\frac{1}{2},r}^n) - F(U_{i-\frac{1}{2},l}^n, U_{i-\frac{1}{2},r}^n)\right)$$

.

Step 3: From $U_j^{n+\frac{1}{2}}$, evaluate the limited slope $\delta U_j^{n+\frac{1}{2}}$ and compute:

$$U_{i-\frac{1}{2},r}^{n+\frac{1}{2}} = U_i^{n+\frac{1}{2}} - \frac{\Delta x}{2}\delta U_i^{n+\frac{1}{2}} \quad \text{and} \quad U_{i+\frac{1}{2},l}^{n+\frac{1}{2}} = U_i^n + \frac{\Delta x}{2}\delta U_i^{n+\frac{1}{2}}$$

.

Step 4: Compute the final solution :

$$U_i^{n+1} = U_i^n - \frac{\Delta t}{\Delta x}\left(F(U_{i+\frac{1}{2},l}^{n+\frac{1}{2}}, U_{i+\frac{1}{2},r}^{n+\frac{1}{2}}) - F(U_{i-\frac{1}{2},l}^{n+\frac{1}{2}}, U_{i-\frac{1}{2},r}^{n+\frac{1}{2}})\right)$$

.

Observe that the step 1 and 2 are identical to step 3 and 4, respectively. Let us focus now on the scheme adapted to a multiphase flow, in particular on the predictor step (steps 1 and 2).

The reconstruction of variables is done on the primitive variables V_i^n, where $V_k = (\alpha_k, \rho_k, u_k, P_k)^T$ for each phase k, because the volume fraction, α, should be between 0 and 1 and because the constraint $\rho_k \geqslant 0$ and $P_k \geqslant 0$. We extrapolate the primitive variables by using their limited slope $\delta_i V$ at most left (l) or right (r) points of the cell $]x_{i-1/2}, x_{i+1/2}[$:

$$V_{i-\frac{1}{2},r}^n = V_i^n - \frac{\Delta x}{2}\delta_i V \quad \text{and} \quad V_{i+\frac{1}{2},l}^n = V_i^n + \frac{\Delta x}{2}\delta_i V$$

.

As a consequence, denoting by $U_{i\pm1/2,r}^n$ (resp. $U_{i\pm1/2,l}^n$) the vector of conservative variables corresponding to $V_{i\pm1/2,r}^n$ (resp. $V_{i\pm1/2,l}^n$), we can write the final formulation of the predictor step, as follows:

$$\frac{W_i^{n+\frac{1}{2}} - W_i^n}{\Delta t} + \frac{\Delta F(W)_i}{\Delta x} = 0 \tag{19}$$

where the arguments are defined by the reconstructed left and right states at $x_{i\pm1/2}$. Since the components of the vector $\Delta F(W)$ should be defined at $x_{i\pm1/2}$, so the components of vector $FT(U_j)$ (see (15)) are defined as follows:

$$\begin{aligned}\mathcal{E}\,(XF)_{i-\frac{1}{2}} =& \mathcal{P}_{i-\frac{1}{2}}(\Sigma_1,\Sigma_1)F(U_{i-\frac{1}{2},l}^{(1),n}, U_{i-\frac{1}{2},r}^{(1),n}) + \\ &+ \mathcal{P}_{i-\frac{1}{2}}(\Sigma_1,\Sigma_2)\left(\beta_{i-\frac{1}{2}}^{(1,2)}\right)F(U_{i-\frac{1}{2},l}^{(1),n}, U_{i-\frac{1}{2},r}^{(2),n}) + \\ &+ \mathcal{P}_{i-\frac{1}{2}}(\Sigma_2,\Sigma_1)\left(\beta_{i-\frac{1}{2}}^{(2,1)}\right)F(U_{i-\frac{1}{2},l}^{(2),n}, U_{i-\frac{1}{2},r}^{(1),n})\end{aligned} \tag{20}$$

$$\begin{aligned}\mathcal{E}\,(XF)_{i+\frac{1}{2}} =& \mathcal{P}_{i+\frac{1}{2}}(\Sigma_1,\Sigma_1)F(U_{i+\frac{1}{2},l}^{(1),n}, U_{i+\frac{1}{2},r}^{(1),n}) + \\ &+ \mathcal{P}_{i+\frac{1}{2}}(\Sigma_1,\Sigma_2)\left(\beta_{i+\frac{1}{2}}^{(1,2)}\right)F(U_{i+\frac{1}{2},l}^{(1),n}, U_{i+\frac{1}{2},r}^{(2),n}) + \\ &+ \mathcal{P}_{i+\frac{1}{2}}(\Sigma_2,\Sigma_1)\left(\beta_{i+\frac{1}{2}}^{(2,1)}\right)F(U_{i+\frac{1}{2},l}^{(2),n}, U_{i+\frac{1}{2},r}^{(1),n})\end{aligned} \tag{21}$$

$$\begin{aligned}\Delta x \left(\mathcal{E}([X]_{j=0})F^{lag}(U_i^-, U_{i-1}^+) - \mathcal{E}([X]_{j=N})F^{lag}(U_i^+, U_{i+1}^-)\right) = \\ = \mathcal{P}_{i+\frac{1}{2}}(\Sigma_1,\Sigma_2)\left(\beta_{i+\frac{1}{2}}^{(1,2),n}\right) F^{lag}(U_{i+\frac{1}{2},l}^{(1),n}, U_{i+\frac{1}{2},r}^{(2),n}) + \\ -\mathcal{P}_{i+\frac{1}{2}}(\Sigma_2,\Sigma_1)\left(\beta_{i+\frac{1}{2}}^{(2,1)}\right) F^{lag}(U_{i+\frac{1}{2},l}^{(2),n}, U_{i+1/2,r}^{(1),n}) + \\ -\mathcal{P}_{i-\frac{1}{2}}(\Sigma_1,\Sigma_2)\left(\beta_{i-\frac{1}{2}}^{(1,2)}\right) F^{lag}(U_{i-\frac{1}{2},l}^{(1),n}, U_{i-\frac{1}{2},r}^{(2),n}) + \\ +\mathcal{P}_{i-\frac{1}{2}}(\Sigma_2,\Sigma_1)\left(\beta_{i-\frac{1}{2}}^{(2,1)}\right) F^{lag}(U_{i-\frac{1}{2},l}^{(2)}, U_{i-\frac{1}{2},r}^{(1)}) + \\ + \max\left(0,\Delta\alpha_i^1\right) F^{lag}(U_i^2, U_i^1) - \max\sum_{N-1}^{l=1}\left(0,\Delta\alpha_i^2\right) F^{lag}(U_i^1, U_i^2),\end{aligned} \tag{22}$$

where $\Delta\alpha_i^1 = \alpha_{i+1/2,l}^1 - \alpha_{i+1/2,r}^1$ and $\Delta\alpha_i^2 = \alpha_{i+1/2,l}^2 - \alpha_{i+1/2,r}^2$ are the limited slope of α^1 and α^2 in the cell C_i. The coefficient $\beta_{i\pm1/2}^{(1,2)}$ represents the sign on the contact speed evaluated at $x_{i\pm1/2}$. For more details, Refs. [14] is strongly recommended.

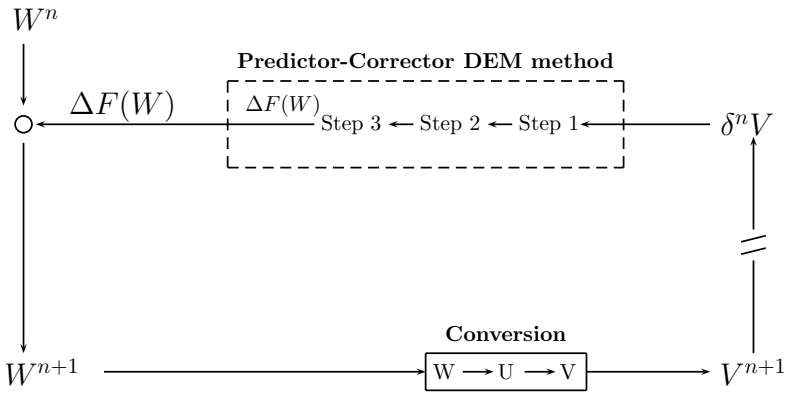

Figure 2: Final sketch of the overall DEM numerical scheme.

In fig. (2), we propose the algoritm in order to compute the solution at the time $n+1$. Let us suppose to know, at the time 0, the primitive variables V, of the seven equation model, that allow to compute the slope *deltaV*. Then, knowning the slope, the evaluate primitive variables in $x_{i\pm+1/2}$ can be computed (step 1) and, then, converted in conservative variables U of the seven equation model in order to compute the fluxes $F(U)$. Following the semi-discrete equation system (13), the conservative variables over half a time step of the five equation system W can be computed (step 2). Converting the conservative variables W in primitive variables of the seven equation system V, using the equation (10) for the mixture pressure, the step 1 and the step 2 must be repeated but evaluating the solution over a whole time step that correspond to the step 3. So, knowing the fluxes $F(U)$ at the time $n+1$, the solution of the five equation system W^{n+1} is computed and converted in primitive variables V^{n+1} in order to restart the cycle.

4 Introducing the stochastic representation in the DEM solver

In this section the stochastic part of the numerical scheme is introduced. In section 4.1 the semi-intrusive approach is briefly described; the introduction of the multiresolution framework, in the semi-intrusive context, is described in the section 4.2 where the adaptive-SI scheme is obtained. Finally the overall numerical scheme, the adaptive-Stochastic Discrete Equation Method aSDEM, is formulated in the section 4.3.

4.1 Generalities on the semi-intrusive approach

The semi-intrusive (SI) approach to the UQ is a novel technique introduced recently by Abgrall and co-workers [**?**, **?**, 26]. The main advantage of the approach is the possibility to obtain very efficient uncertainties propagation in virtually any kind of numerical scheme without any kind of limitation related to the distribution of the uncertainties parameters. In particular discontinuous and time-varying pdf can be employed in a straightforward manner. The approach belongs to the so-called *intrusive* class because requires the modification of an existing numerical code, however these modification are all contained in the numerical implementation part and not in the theoretical framework as, for instance, required by the intrusive PC. The SI approach even if intrusive results to be very flexible as well as a non-intrusive approach. In the following the key elements of the approach are outlined supposing, for simplicity of exposure, to apply the approach to a scalar conservation law. This simplification does not introduce any limitation and it will be retained also in the section 4.2 where the adaptive version of the SI scheme is presented. However in section 4.3 the overall numerical scheme relative to the multiphase problem is described in more details highlighting its key elements. However the reader should refer to [26] for further details on the semi-intrusive approach.

Let consider the following scalar conservation laws, governing the quantity $u = u(x, t, \xi)$

$$\frac{\partial u(x,t,\xi)}{\partial t} + \frac{\partial u(x,t,\xi)}{\partial x} = 0, \tag{23}$$

where $x \in \Omega \subset \mathbb{R}$ is the physical space, $t \in T \subset \mathbb{R}^+$ the time space and $\xi \in \Xi \subset R$ the stochastic space with a proper probability distribution $p(\xi)$. A proper initial condition $u_0 = u(x, 0, \xi)$ and boundary condition are supposed to be assigned for the well definition of the problem. A first order Godunov method (that can be viewed as the predictor or corrector step of the MUSCL scheme described for the solution of the DEM scheme) employing a FV cell tessellation for the physical space $\Omega = \bigcup_{i=1}^{N_x} \mathcal{C}_i$ and a constant subdivision of the time space $t_n = n\Delta t$ is

$$\bar{u}_i^{n+1}(\xi) = \bar{u}_i^n(\xi) + \frac{\Delta t}{|\mathcal{C}_i|}\left(F(\bar{u}_{i-1}^n(\xi), \bar{u}_i^n(\xi), \xi) - F(\bar{u}_i^n(\xi), \bar{u}_{i+1}^n(\xi), \xi)\right), \tag{24}$$

where $\bar{u}$ indicates the spatial cell average while $F(\bar{u}_{i-1}^n(\xi), \bar{u}_i^n(\xi), \xi)$ and $F(\bar{u}_i^n(\xi), \bar{u}_{i+1}^n(\xi), \xi))$ are the numerical flux functions at the left and right interfaces as usual.

The semi-intrusive approach is based on a tessellation of the stochastic space employing the measure μ associated to the probability density function $p(\xi)$

$$\Xi = \bigcup_{j=1}^{N_\xi} \Xi_j, \quad \text{with} \quad \mu(\Xi_i \cap \Xi_j) = 0 \quad \text{if} \quad i \neq j, \tag{25}$$

where the measure of a generic stochastic cell Ξ_j is

$$\mu(\Xi_j) = \int_{\Xi_j} p(\xi) \mathrm{d}\xi = \int_{\Xi_j} \mathrm{d}\mu > 0. \tag{26}$$

On each generic stochastic cell Ξ_j a conditional expectancy operator, applied to the spatial cell average $\bar{u}_i$, can be defined as

$$\mathbb{E}\left(\bar{u}_i^n \,|\, \Xi_j\right) = \frac{1}{\mu(\Xi_j)} \int_{\Xi_j} \bar{u}_i^n(\xi)\, p(\xi) \mathrm{d}\xi. \tag{27}$$

If the conditional expectancy operator is applied to the equation (24) the final scheme semi-intrusive scheme is obtained as

$$\mathbb{E}\left(\bar{u}_i^{n+1} \,|\, \Xi_j\right) = \mathbb{E}\left(\bar{u}_i^n(\xi) \,|\, \Xi_j\right) + \frac{\Delta t}{|\mathcal{C}_i|} \left(\mathbb{E}\left(F(\bar{u}_{i-1}^n(\xi), \bar{u}_i^n(\xi), \xi) \,|\, \Xi_j\right) - \mathbb{E}\left(F(\bar{u}_i^n(\xi), \bar{u}_{i+1}^n(\xi), \xi) \,|\, \Xi_j\right) \right). \tag{28}$$

The computation of the statistics (for instance the variance or the pdf) of the output $\bar{u}$, and also the evaluation of the expectancies of the fluxes, $\mathbb{E}\left(F(\bar{u}_{i-1}^n(\xi), \bar{u}_i^n(\xi), \xi) \,|\, \Xi_j\right)$ and $\mathbb{E}\left(F(\bar{u}_i^n(\xi), \bar{u}_{i+1}^n(\xi), \xi) \,|\, \Xi_j\right)$, can be performed only knowing the values of the spatial cell average over each cell. This task is accomplished introducing the conservative reconstruction step as in the classical FV scheme. In particular a polynomial $P_j(\xi)$, of degree r, with $\xi \in \Xi_j$ can be determined on each cell Ξ_j by requiring

$$\mathbb{E}\left(P_j \,|\, \Xi_l\right) = \mathbb{E}\left(\bar{u}_i^n \,|\, \Xi_l\right) \quad \text{with} \quad \Xi_l \in \mathcal{S}_j, \tag{29}$$

where $\mathcal{S}_j$ is a proper stencil subjected to a Vandermonde-like condition and dependent from the degree of the polynomial approximation. For instance the cardinality of $\mathcal{S}_j$ in a 1D context is equal to $r + 1$. Knowing the conditional expectancy of the solution on each cell is equivalent, through the reconstruction step, to the knowledge of the solution over the entire stochastic space Ξ. The computation of the expectancies of the fluxes is finally performed injecting the polynomial P_j. The details on the computation of the fluxes are furnished in the section 4.3 for the overall scheme. In the following section a multiresolution version of the semi-intrusive scheme, here introduced, is presented. This MR approach has already been demonstrated to increase the computational efficiency of the semi-intrusive scheme in its basic form (see for instance [27]).

4.2 The multiresolution version of the SI scheme: the adaptive-SI method

In this section the multiresolution of the SI scheme is briefly described. The basic element is the Truncate and Encode (TE) multiresolution framework presented in [35]. The TE framework is employed to perform a hierarchical refinement of

the stochastic space employing the wavelets as error estimators. This framework has been already introduced in the SI scheme in [27] while in this paper is employed as a building block of a novel and efficient intrusive stochastic scheme for multiphase problems in which the so-called Discrete Equation Method is adopted. The MR framework is introduced only for the representation of the solution in the stochastic space, but as it will be evident, it is enough to obtain a time dependent adaptivity of the tessellation in the combined physical-stochastic space.

The aim of introducing the MR framework is twofold. First, for compressible CFD problems, the propagation of narrow discontinuity region is a common issue. The MR basis offers a natural compact representation of this kind of functions, as already demonstrated in the seminal papers of Harten [41, 42, 43]. Moreover, another interesting feature of the MR is the possibility to analyze locally the regularity of a function. This feature can be employed to drive a topological refinement of the mesh in a time-dependent way. The multiresolution framework is based on different (discrete) resolution levels k with increasing resolution as k increase, *i.e.* $k = 0$ is the lower resolution level and $k = L$ is the higher. Each continuous function $u \in \mathcal{F}$, where $\mathcal{F}$ is a proper functional space, can be discretized on kth discrete resolution level and is designed as v^k. The multiresolution framework is based on different operators performing mapping between the continuous space and the discrete resolution levels. These operators are recalled in the following. First, the discretization operator $\mathcal{D}_k$ features the mapping between the continuous space of definition of the function in the analysis and discrete tessellation of resolution level k. The inverse operation is performed by a reconstruction operator $\mathcal{R}_k$. It is clear that the two operators should be consistent, *i.e.* $\mathcal{R}_k\mathcal{D}_k = I$. Moreover, operations between discrete levels are also demanded. The decimation operator D_k^{k-1} allows obtaining a coarser level from a finer one, while the prediction operator is designed to predict the value of a discrete element, for instance a cell-average, from a coarser resolution level. The role played by each of these operator is sketched in the figure 3.

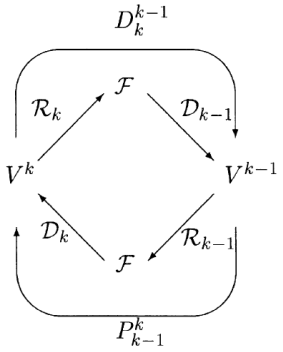

Figure 3: Sketch of the role played by the operators $\mathcal{D}_k$, $\mathcal{R}_k$, D_k^{k-1} and P_{k-1}^k between the discrete and continuous spaces. Figure reproduced from [**?**].

In the MR context the linear independent components of the error, between the prediction and the exact solution, for each resolution level, are called

wavelets and they are defined as

$$d^k = v^k - \mathrm{P}^k_{k-1} v^{k-1}. \tag{30}$$

The TE framework is based on the recursive discretization of the solution from the coarser to the finest level where the refinement is performed locally only if the local error is greater than a prescribed threshold, *i.e.* if the local wavelet $d^k_j > \varepsilon_k$. In this work the law of variation of the threshold is defined as $\varepsilon_k = \varepsilon/2^{L-k}$.

The link between the SI scheme and the TE framework is constituted by the reconstruction operator $\mathcal{R}_k$. The reconstruction operator can be defined as the union of all the conservative polynomials P_j over each stochastic cell Ξ_j:

$$\mathcal{R}_k(\xi) = P_j(\xi) \quad \text{for} \quad \xi \in \Xi_j. \tag{31}$$

In the following section the overall adaptive-Stochastic Discrete Equation Method is presented highlighting the interaction between the DEM and the aSI techniques.

4.3 The aSDEM overall numerical scheme

The aSI scheme, as sketched in the previous section, is based on hierarchical (recursive) evaluation of the discrete resolution levels. Each resolution level is constituted by a succession (even non-regular) of stochastic cells on which the conditional expectancies of the solution are evaluated.

Let consider a fixed physical location, for a generic resolution level k, a tessellation of the stochastic space is

$$\Xi = \bigcup_{j=1}^{N^k_\xi(x,t)} \Xi^k_j, \quad \text{with} \quad \mu(\Xi^k_i \cap \Xi^k_j) = 0 \quad \text{if} \quad i \neq j. \tag{32}$$

Let now suppose to consider the final step (19) and to apply the conditional expectancy operator on the generic kth level. For each generic cell Ξ^k_j of the tessellation, the final step (19), for the corrector, becomes

$$\mathbb{E}\left(W^{n+1}_i \,|\, \Xi^k_j\right) = \mathbb{E}\left(W^n_i \,|\, \Xi^k_j\right) + \frac{\Delta t}{\Delta x}\mathbb{E}\left(\Delta F(W)_i \,|\, \Xi^k_j\right). \tag{33}$$

The time-update, reported in Eq. (33), concerns the time-advancing strategy to increment the conditional expectancy of the solution, in a generic cell Ξ^k_j, by knowing its value at the previous time step and the expectancy of the fluxes at the interfaces. Let us imagine to formulate an initial value problem, *i.e.* a differential problems in which the initial condition is known. If a proper quadrature rule is chosen, in the combined physical-stochastic space, the value of the conditional expectancy of the initial solution can be obtained. The remaining step is to compute the computational expectancy of the fluxes. At this level, the interaction of the aSI formulation with the deterministic is evident. In the particular case of DEM method (see the previous sections), solved by a predictor-corrector approach, it is possible to compute the value of the vector of conservative variables in a cell $\mathcal{C}_i$, knowing only the solutions at the cells $\{\mathcal{C}_{i-3}, \ldots, \mathcal{C}_{i+3}\}$. This derives from the need to compute a half time updated

solution (for the predictor) in the cells $\{\mathcal{C}_{i-2},\dots,\mathcal{C}_{i+2}\}$, and then applying the corrector (on the updated values) on the cell $\{\mathcal{C}_{i-1},\dots,\mathcal{C}_{i+1}\}$. Remark that the computation of the slopes yields the enlargement of the stencil of one cell for side. The predictor step can be performed after that the local physical cell-averages are computed. In principle, the scheme handles only conditional expectancy. By means of the reconstruction operator $\mathcal{R}_k$ of the MR framework, the physical cell average values, for the stencil $\{\mathcal{C}_{i-3},\dots,\mathcal{C}_{i+3}\}$ are evaluated. The problem is equivalent to the deterministic one: the seven physical cell-average values are updated of half time step and the extrapolated values at the interfaces, of the cell of interest, can be computed. If this procedures is performed for all the Ng quadrature points of each physical interfaces, between spatial cells along the stochastic coordinate, the quadrature of the term ΔF can be easily obtained. The final step (33) can be finally applied. In the Algorithm 4, the set of operation, to compute the difference of the fluxes expectancies, is reported.

Algorithm 1: Computation of the fluxes expectancies in the aSI scheme for the DEM formulation with a predictor-corrector MUSCL approach.

for ng = $1,\dots,$Ng **do**

- Physical Vector PV assembling:
  Conservative reconstruction from $\mathbb{E}\left(W_i^n \,|\, \Xi_j^k\right)$ by MR reconstruction operator $\mathcal{R}_k$
  Conversion in primitive variables (of the 7 equation model): from U_i to V_i

  $$\mathrm{PV}(\boldsymbol{\xi}_{\mathrm{ng}}) = \left\{V_{i-3}^n(\boldsymbol{\xi}_{\mathrm{ng}}),\dots,V_{i+3}^n(\boldsymbol{\xi}_{\mathrm{ng}})\right\}$$

- Imposition of the boundary conditions
- Slope computations (and limiting) $\forall \mathcal{C}_\ell \in \{\mathcal{C}_{i-2},\dots,\mathcal{C}_{i+2}\}$:

  $$\delta_\ell^n(\boldsymbol{\xi}_{\mathrm{ng}}) = \delta\left(V_{\ell-1}^n(\boldsymbol{\xi}_{\mathrm{ng}}), V_\ell^n(\boldsymbol{\xi}_{\mathrm{ng}}), V_{\ell+1}^n(\boldsymbol{\xi}_{\mathrm{ng}})\right)$$

- Extrapolation $\forall \mathcal{C}_\ell \in \{\mathcal{C}_{i-3},\dots,\mathcal{C}_{i+3}\}$ (*Step 1*)
- Semi-time step evolution $\forall \mathcal{C}_\ell \in \{\mathcal{C}_{i-2},\dots,\mathcal{C}_{i+2}\}^a$ (*Step 2*):
- Extrapolation $\forall \mathcal{C}_\ell \in \{\mathcal{C}_{i-1},\dots,\mathcal{C}_{i+1}\}$ (*Step 3*)
- Delta flux computation: $\Delta F(W(\boldsymbol{\xi}_{\mathrm{ng}}))_i$ (DEM solver)

end

Flux Quadrature:

$$\mathbb{E}\left(\Delta F(W)_i \,|\, \Xi_j^k\right) = \sum_{i=\mathrm{ng}}^{\mathrm{Ng}} w_{\mathrm{ng}} \Delta F(W(\boldsymbol{\xi}_{\mathrm{ng}}))_i$$

Figure 4: Algorithm 1

Once the time-update step (33) is formulated, this step can be considered as the result of the application of the discretization operator in MR. This step, for each stochastic cell Ξ_j, corresponding to a fix spatial location, is represented in the figure 5. Performing, at each time step and for each physical coordinate, a MR driven refinement/derefinement (using the discretization operator $\mathcal{D}_k$ or relying only on prediction by P_{k-1}^k), the compact (with respect to the discrete dimensionality) representation of each conservative variable can be obtained. The final step of the UQ propagation process is the computation of statistics. They can be computed, even analytically, knowing the reconstruction operator in each cell along the stochastic coordinates. In this paper, the numerical test cases are carried out introducing a non-linear Essentially Non-Oscillatory (ENO) reconstruction based on cubic polynomials. The advantage of a such re-

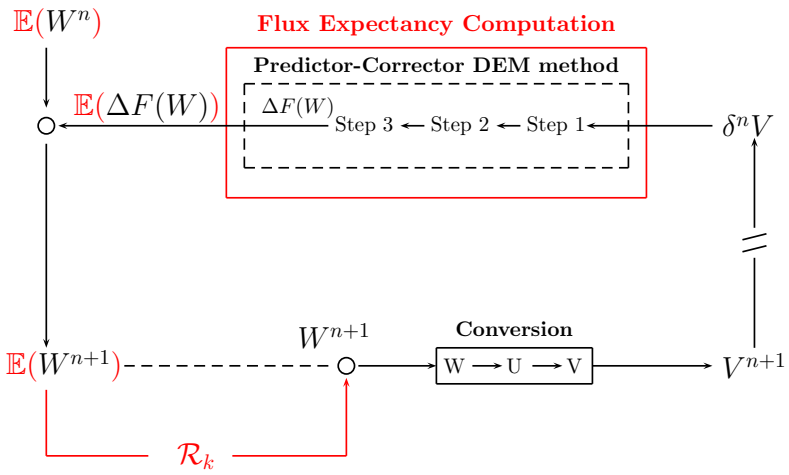

Figure 5: Final sketch of the overall aSDEM numerical scheme.

construction technique, in the context of the MR approach proposed here, have been already shown in papers [44, 27].

4.3.1 Extension to the multiphase vectorial case

In the previous section the MR framework has been introduced to drive the topological refinement of the mesh over the stochastic space. The refinement/derefinement is performed employing as indicator the wavelets d^k on each kth resolution level. The refinement/derefinement is performed on the vector of conservative variables regarding the five equations problem W (see equation (18)). The general procedure to extend the application of the TE framework to vectorial problems requires to compute the greater wavelet with respect the ones relative to each component of the conservative vector W. The order of magnitude of each component is different in a general case and the wavelets for each component of W need to be scaled with respect to a reference value. In particular, in this work, the following procedure is adopted. A set of fixed variables is chosen: $\bar{\alpha_1}$, $\bar{\rho_1}$, $\bar{\rho_2}$, $\bar{u}_1$, $\bar{u}_2$, $\bar{P}_1$ and $\bar{P}_2$.

A vector of reference conservative variable is then obtained as

$$W = \bar{W} = \begin{pmatrix} \bar{\alpha_1} \\ \bar{\alpha_1}\bar{\rho_1} \\ (1-\bar{\alpha_1})\bar{\rho_2} \\ \bar{\alpha_1}\bar{\rho_1}\bar{u}_1 + (1-\bar{\alpha_1})\bar{\rho_2}\bar{u}_2 \\ \bar{\alpha_1}\bar{\rho_1}\bar{E}_1^t + (1-\bar{\alpha_1})\bar{\rho_2}\bar{E}_2^t \end{pmatrix} \tag{34}$$

where the velocities are set equal to the relative speed of sound of the kth phase

$$\bar{u}_k = \sqrt{\frac{\gamma_k(\bar{P}_k - P_{k,\infty})}{\bar{\rho}_k}} \tag{35}$$

and the reference total energy is

$$\bar{E}_k^t = \frac{\bar{P}_k + P_{k,\infty}\gamma_k}{(\gamma_k - 1)\bar{\rho}_k} + \frac{1}{2}\frac{\gamma_k(\bar{P}_k - P_{k,\infty})}{\bar{\rho}_k}. \tag{36}$$

		Constant Fluid Conditions		
		γ	P_∞	$u_L = u_R$ $[m/s]$
All TC	Liq	4.4	6×10^9	0
	Gas	1.4	0	

n	Fluid	Test Case (TC) conditions						Uncertainty
		Left			Right			
		α	$\rho\ [\frac{kg}{m^3}]$	P [Pa]	α	$\rho\ [\frac{kg}{m^3}]$	P [Pa]	
TC1	G=Air	1-ϵ	$\rho_G(\xi)$	1.0	1-ϵ	0.125	0.1	$\rho_G(\xi) = 0.3 + 1.6\xi$
	L=Water	ϵ	1000		ϵ	1000		
TC2	G=Air	$\alpha_G(\xi)$	50	1.0E+9	50	50	1.0E+5	$\alpha_G(\xi) = \alpha_G \pm 0.1\xi$
	L=Water	$1-\alpha_G(\xi)$	1000		0.5	1000		
TC3	G=Air	0.2	1	$P_{Left}(\xi)$	0.8	1	1.0E+5	$P_{Left}(\xi) = (0.95 \pm 0.1\xi) \times 10^9$
	L=Water	0.8	1000		ϵ	1000		

Table 2: Initial conditions for all test cases. $\epsilon = 10^{-8}$. For all test cases, in the right and left part, u_k=0.

The final selection of the wavelet is made dividing each wavelet by the reference value of the conservative component:

$$d^k = \max(d_1^k/\bar{W}_1, \ldots, d_5^k/\bar{W}_5). \tag{37}$$

In all the computations performed in this work the reference variables are selected taking the unperturbed values at the left side of the shock tube. In the case of a stochastic variable associated to the reference value, this last is set equal to the expected value of the input variable.

5 Results

In this section, we show the results obtained for three test cases. Initial conditions and working fluids are specified for each test-case and summarized in table 2.

First, the implementation of the scheme is validated by running a stochastic test case well known in literature, for which the exact solution can be computed in the stochastic and physical spaces.

The other test-cases deals with a two-phase shock tube using a mixture of air and water as working fluid. Influence of uncertainty on the left gas volume fraction and on the left pressure, is investigated. Moreover stochastic and grid convergence are explored in different conditions.

5.1 TC1: validation of the scheme in a quasi-single phase fluid

The original test case [27] reproduces a single-phase (air) shock tube where the density on the left state is dependent on an uniformly distributed random parameter ξ. This test case is of interest since the exact solution in the stochastic space can be computed [27], thus, permitting to estimate scheme convergence. In particular, in this work, we consider a quasi single-phase shock tube, *i.e.* a mixture of air and water, where in each chamber of the tube a reduced liquid

fraction is supposed (typically 10^{-8}).
This test-case has been modified in this sense for two different reasons:

- in order to verify that the coupling works well, *i.e.* that global stochastic/physical scheme is sufficiently robust to capture two-phase flow, eve, with a very reduced liquid fraction.
- Accuracy in the stochastic space can be assessed by making a comparison with respect to the exact solution (hypothesis that stochastic solution in a single-phase or quasi-single fluids are very similar).

Initial conditions of this test case are specified in table 2. Left and right sides of the shock tube are filled out, principally, with air ($\alpha_{air} = 1 - 10^{-8}$) and with a very low percentage of water ($\alpha_{water} = 10^{-8}$). Density on the left state is dependent on an uniformly distributed random parameter $\xi \sim \mathcal{U}[0,1]$: $\rho_L(\xi) = 0.3 + 1.6\xi\ kg/m^3$. Values of the pressures are $p_L = 1$ and $p_R = 0.1$, while the right value of the density is $\rho_R = 0.125$. Simulations are performed over a physical domain $\Omega = [-\frac{1}{5}, \frac{6}{5}]$ until a final time $t = 0.31$ with the position of the diaphragm equal to $x_d = 0.42$. The time space is divided in 6200 equal time steps of length $\Delta t = 5 \times 10^{-5}$.

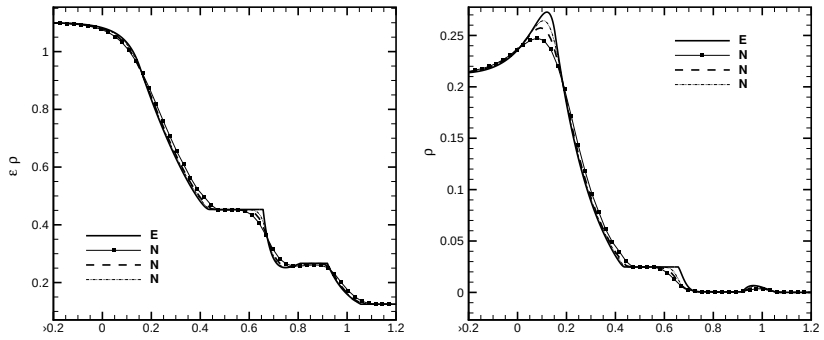

(a) (b)

Figure 6: Evolution of the density expectancy (a) and density variance (b) for the cell averaged solution of an uncertain shock tube problem at the final time $t = 0.31$ and for different physical meshes.

Simulations are carried out over equally spaced meshes of 51, 101, 201 points employing the aSI scheme based on the MUSCL method (see 3.1 section) with a Superbee limiter.

In figure 6, the evolution of the density expectancy and density variance are reported. Note that the exact solution is reported over a mesh of 2001 equally spaced points in the physical space. As it is evident, by increasing the number of points in the physical space, stochastic solution converge to the exact one, for both mean and variance.

In figure 7, the spatial convergence is reported for both the mean and the variance in L^1 and L^2 for the density ρ. The aSI method is obtained with a level of 128 ($m = 7$) stochastic cells with $\varepsilon = 10^{-4}$, while the reference solution is the exact solution obtained in [27].

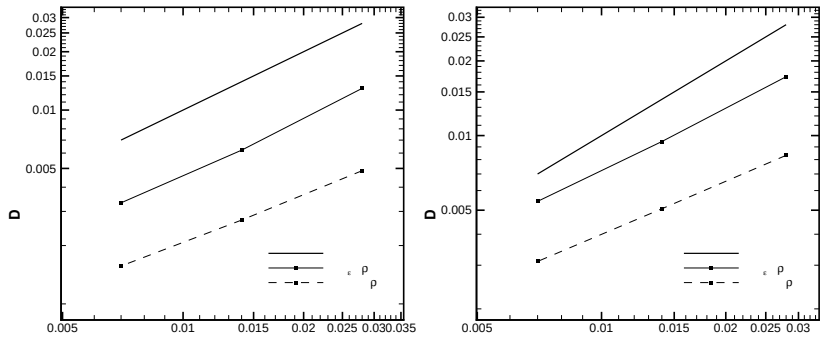

(a) (b)

Figure 7: Spatial convergence for the stochastic shock tube problem with density uncertain initial condition [27]. L^1 (a) and L^2 (a) norms are shown for the statistic (mean and variance) of the solution.

5.2 TC2: two phase flow with uncertainty on gas volume fraction

In this case, the shock tube is filled out with water and air at the same volume fraction ($\alpha_k = 0.5$) on the right and on the left of diaphragm, located at x=0.5m. Initial conditions of this test case are described in the table 2. The deterministic solution has been validated in [17].
The gas volume fraction on the left state is dependent on an uniformly distributed random parameter $\xi \sim \mathcal{U}[0,1]$: $\alpha_G(\xi) = \alpha_G \pm 0.1\xi$ and its propagation in the shock tube is observed. Simulations are performed over a physical domain $\Omega = [0,1]$ until a final time $t = 193.744\ \mu s$. The time space is divided in 1900 equal time steps of length $\Delta t = 1 \times 10^{-7}$. The simulations are carried out over equally spaced meshes of 101, 201, 401 and 801 points employing the aSI scheme based on the MUSCL method with a Van Leer limiter.

In figure 8(a), the spatial convergence is reported for both the mean and the variance in L^1 for the density ρ. It has been obtained with the aSI method with a level of 128 ($m = 7$) stochastic cells. Results obtained by the aSI method have been compared with the ones obtained by a full SI scheme, in terms of L1 norm (figure 8(b)) and of density mean and variance curves (figure 9), showing a perfect overlapping of the curves. For this reason, since we observed for all computations the same behavior of both the methods, hence, the figures and the observations will be presented only the aSI scheme results.

The figures 10 and 11 show the deterministic spatial convergence in terms of mean and variance carried out over equally spaced meshes of 101, 201, 401 and 801 points employing the aSI scheme with a level of 512 ($m = 9$) stochastic cells.The most significant differences can be observed on the liquid and gas densities for both the statistics (mean and variance) of the solution (see figures 10(c)-10(d) and 11(c)-11(c)). The coarser mesh shows a behavior very different compared with the finest mesh for $0.6 < x < 0.75$, corresponding to the contact discontinuity and the shock wave.

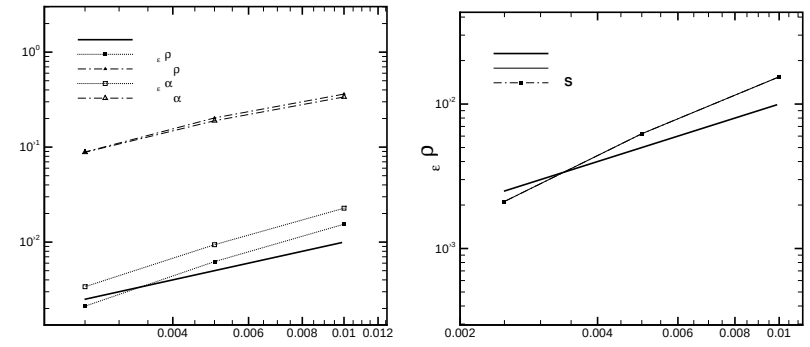

(a) (b)

Figure 8: (a) Spatial convergence for the stochastic shock tube problem with an uncertain volume fraction as initial condition. L1 norms are shown for the density expectancy and variance of the solution.(b) Comparison between aSI and full SI scheme obtained with a level of 128 (m=7) is shown on the stochastic spatial convergence of the density expectancy.

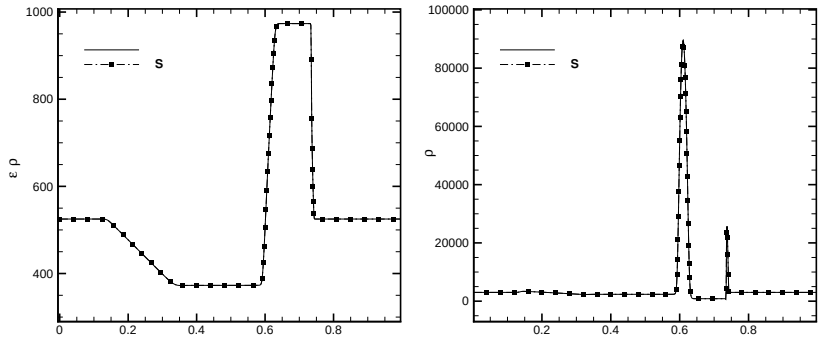

(a) (b)

Figure 9: Comparison between aSI and full SI scheme obtained with a level of 128 (m=7) on a deterministic space grid of 801 points, for (a) density expectancy and (b) density variance.

The scheme allows to evaluate clearly the propagation of uncertainty and with this test case we study the influence of inlet left gas volume fraction, α_g. Observing the variance profiles of thermodynamic variables, all of them present a pick in correspondence to the shock (see figure 11), but the phase density profiles and, of course, the gas volume fraction profile show a significant variation in correspondence to $x = 0.6$ m (see figure 11(a)-11(d)). These differences are more evident in figure 12, where the mean and standard deviation curves are compared on all the deterministic space. It is evident that the pressure is not influenced by the uncertainties. On the contrary, the phase densities profiles

change especially in correspondence to $0.6 < x < 0.75$ (see figures 12(c) and 12(d)), while the inlet uncertainty influence the gas volume fraction behavior before and after the shock (see figure 12(a)).

5.2.1 TC3: two-phase flow with pressure uncertainty

The last test case has been proposed in [1] and it reproduces a two-phase shock tube with initial conditions summarized in table 2. Simulations are performed over a physical domain $\Omega = [0, 1]$ until a final time t=200 μs. The time space is divided in 20000 equal time steps of length $\Delta t = 1 \times 10^{-8}$. The simulations are carried out over equally spaced meshes of 101, 201, 401 and 801 points employing the aSI scheme based on the MUSCL method with a VanLeer limiter.
An uncertainty of 5% is supposed for the initial left pressure and its propagation in the shock tube is observed.

In figure (13), the spatial convergence is reported for both the mean and the variance in L^1 for the mixture density ρ and the gas volume fraction α_g. It has been obtained with the aSI method with a level of 512 ($m = 9$) stochastic cells.

Figures 14 and 11 show the deterministic spatial convergence in terms of mean and variance carried out over equally spaced meshes of 101, 201, 401 and 801 points employing the aSI scheme with a level of 512 ($m = 9$) stochastic cells. The most significant differences between the coarsest and the finest meshes in term of gas density and gas volume fraction in correspondence to $0.8 < x < 0.9$ m (see figures 14(a) and 14(c)). In this test-case, we study the influence of inlet left pressure variation. On the contrary of previous case, the profiles of all thermodynamic variables do not show a significant variation of curves, except in correspondence of shock (see figures 15 and 16).

6 Conclusions

This paper deals with a scheme for simulating stochastic two-phase compressible flows. This scheme relies on a DEM formulation, but reformulated for including an adaptive semi-intrusive scheme (aSI), thus efficiently capturing the propagation of uncertainties. Several test-cases have been investigated. In particular, shock tube configuration has been considered in order to explore the stochastic and grid convergence in different conditions. This scheme displays good convergence properties in each test case for both stochastic and physical spaces. Convergence curves are shown in the physical and stochastic spaces, respectively. Moreover, the variability (in terms of mean and standard deviation) of several properties, such as density, pressure and velocity is computed by considering different kinds of uncertainty, *i.e.* on the initial volume fraction, density or pressure.

Thanks to the robustness of the scheme and to its ability to solve the interface problems, this scheme will be extended to a multi-dimensions investigation in the stochastic and physical spaces.

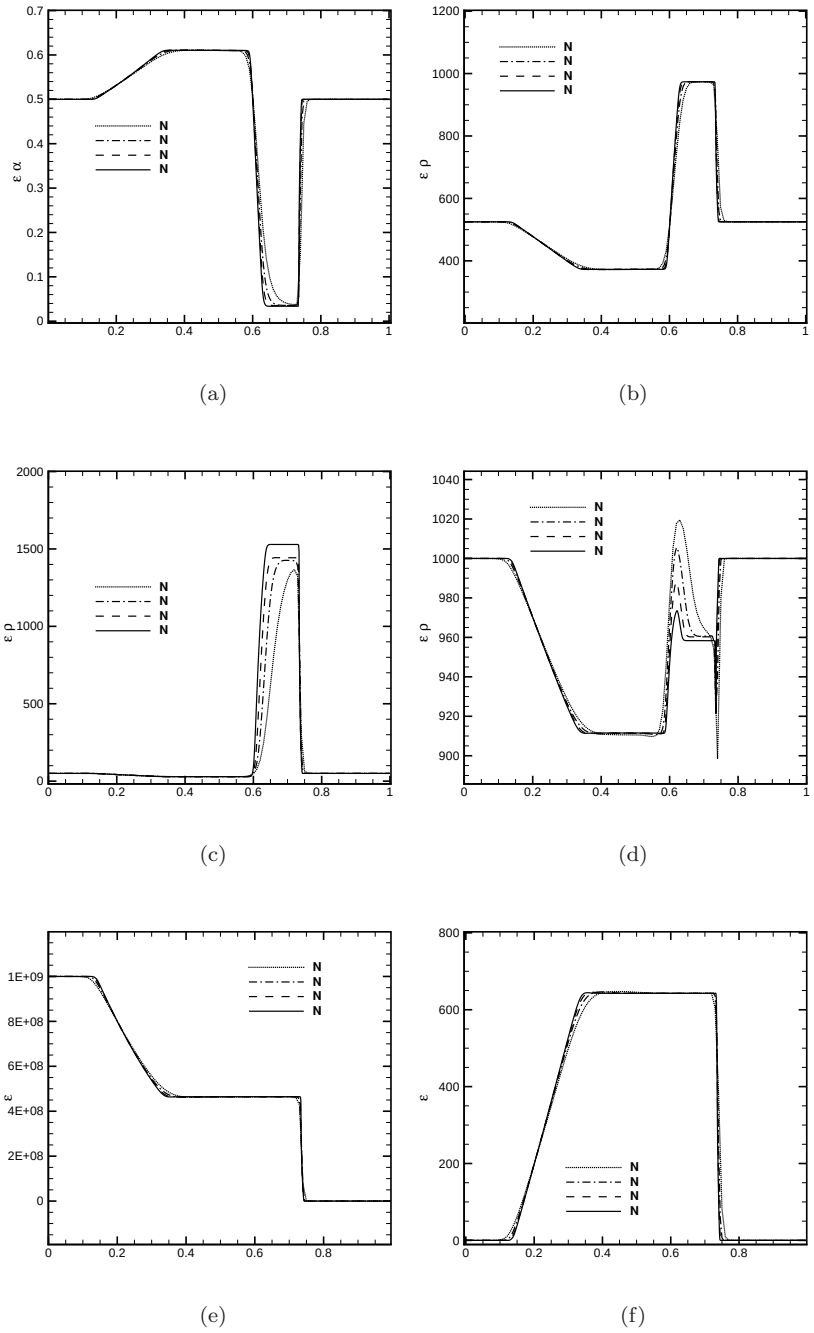

(a) (b)

(c) (d)

(e) (f)

Figure 10: Deterministic spatial convergence of the expectancy for the (a) gas volume fraction, (b) mixture density, (c) gas density, (d) liquid density, (e) mixture pressure and (f) mixture velocity. aSI scheme obtained with a level of 512 (m=9).

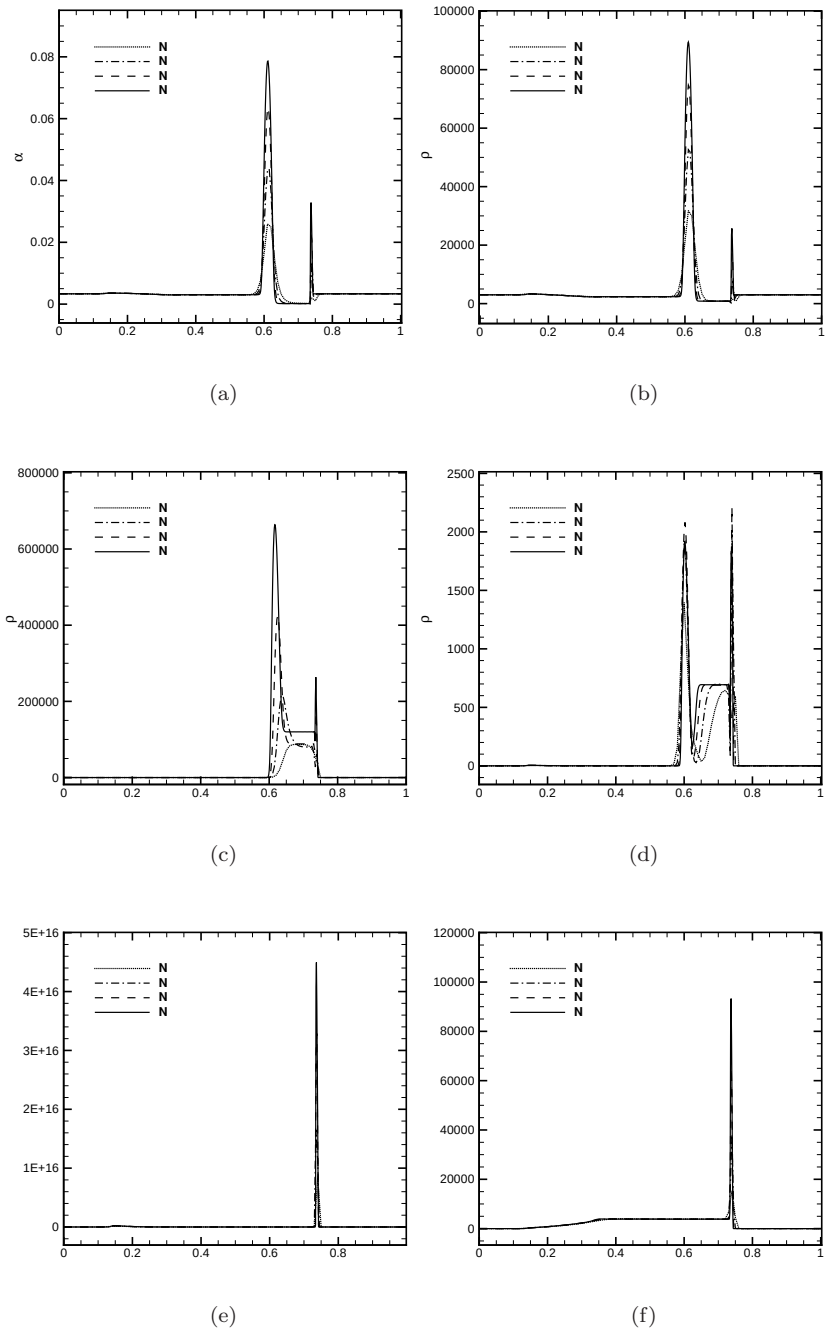

Figure 11: Deterministic spatial convergence of the variance for (a) gas volume fraction, (b) mixture density, (c) gas density, (d) liquid density, (e) mixture pressure and (f) mixture velocity. aSI scheme obtained with a level of 512 (m=9).

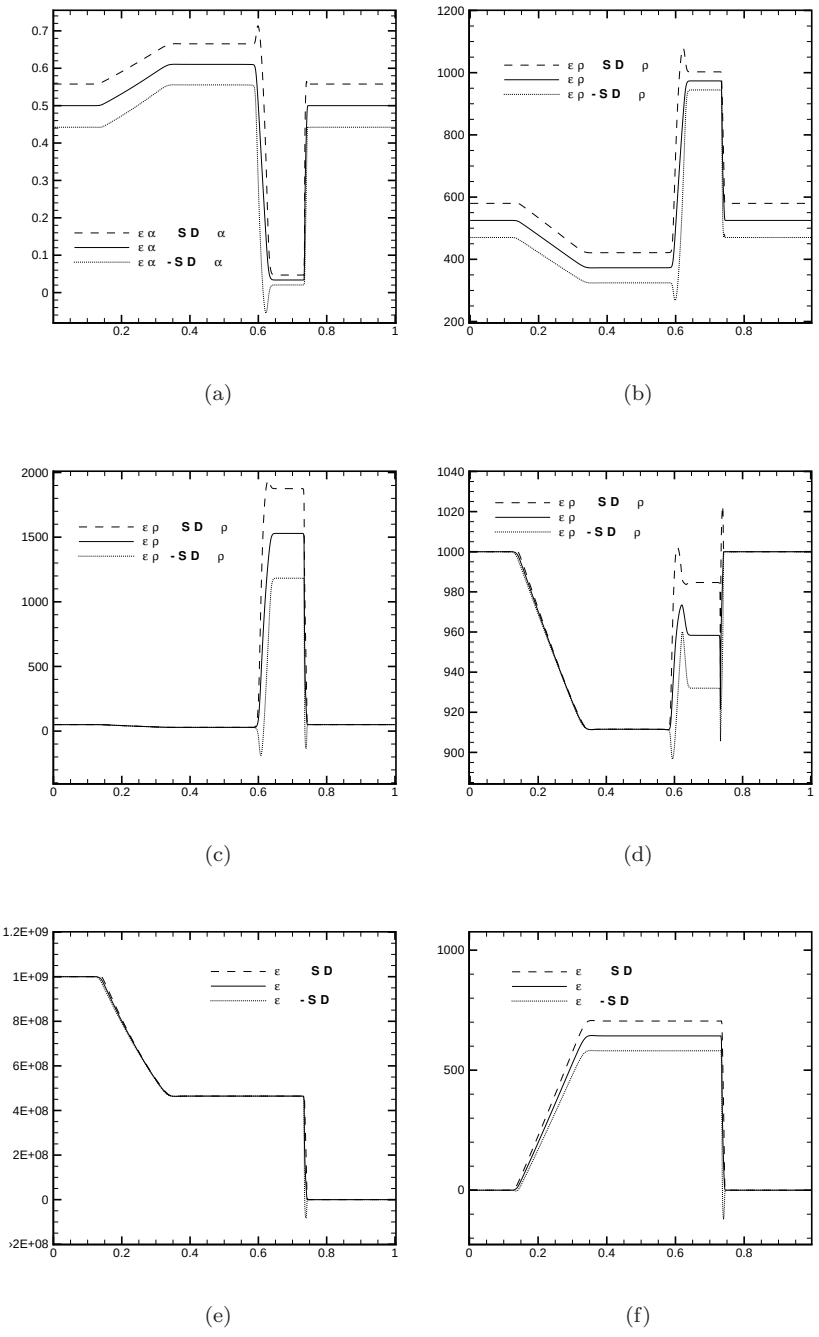

Figure 12: Confidence intervals ($\mu \pm \sigma$) for (a) gas volume fraction, (b) mixture density, (c) gas density, (d) liquid density, (e) mixture pressure and (f) mixture velocity. aSI scheme obtained with a level of 512 (m=9).

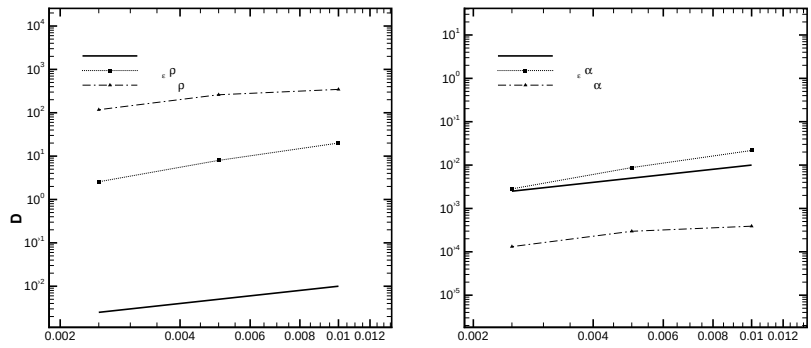

(a) (b)

Figure 13: Spatial convergence for the stochastic shock tube problem with an uncertain pressure as initial condition. L1 norms are shown for the density (a) and volume fraction (b) expectancy and variance of the solution. aSI scheme obtained with a level of 512 (m=9).

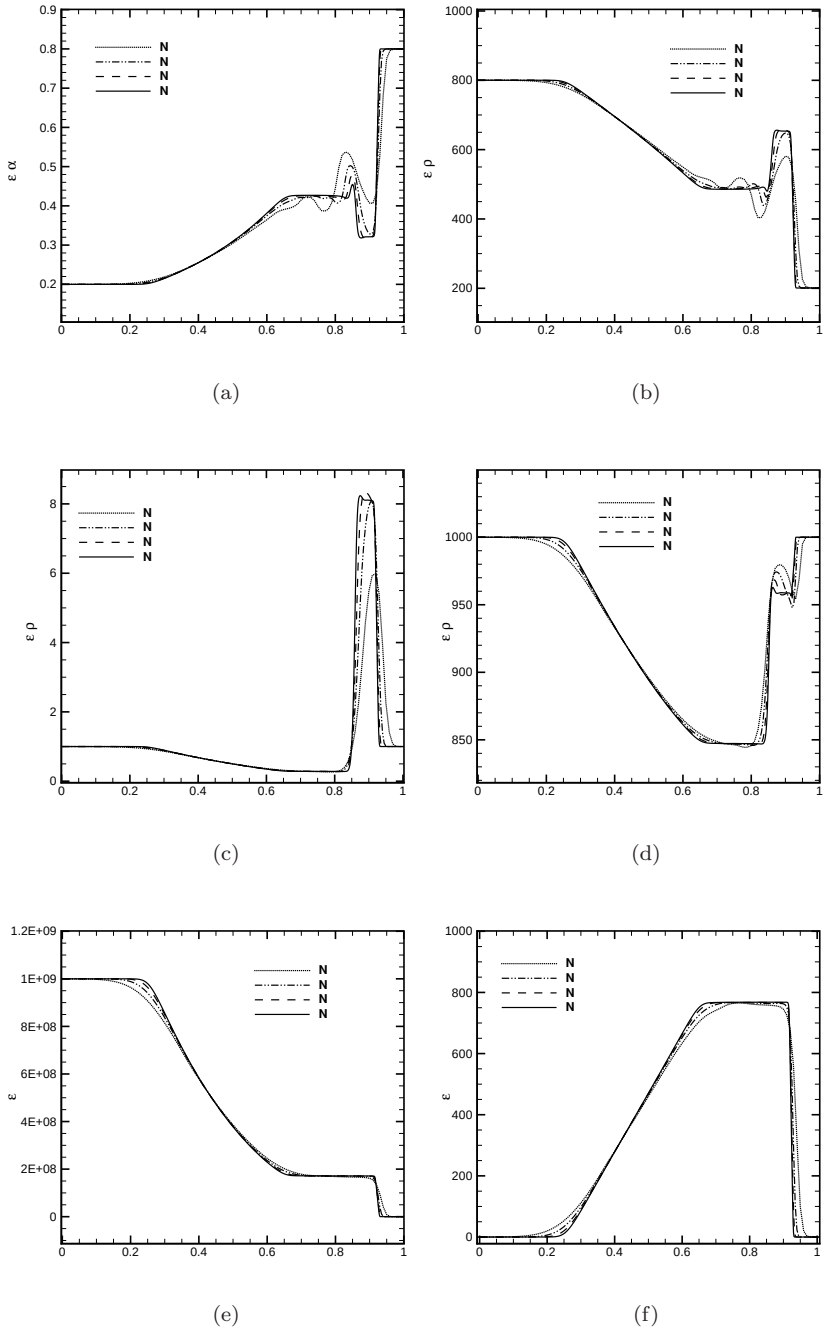

(a) (b)

(c) (d)

(e) (f)

Figure 14: Deterministic spatial convergence of the expectancy for (a) gas volume fraction, (b) mixture density, (c) gas density, (d) liquid density, (e) mixture pressure and (f) mixture velocity. aSI scheme obtained with a level of 512 (m=9).

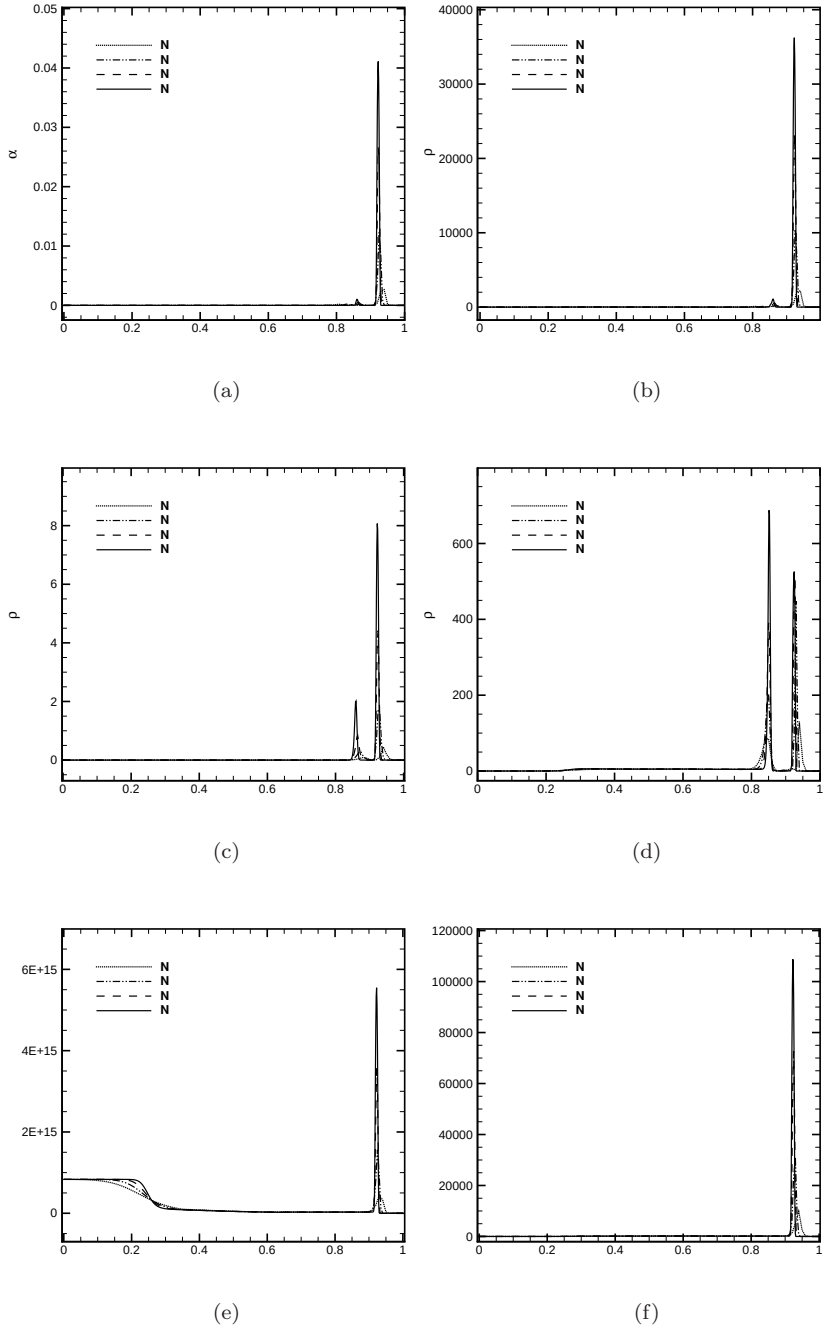

Figure 15: Deterministic spatial convergence of the variance for (a) gas volume fraction, (b) mixture density, (c) gas density, (d) liquid density, (e) mixture pressure and (f) mixture velocity variance, respectively. aSI scheme obtained with a level of 512 (m=9).

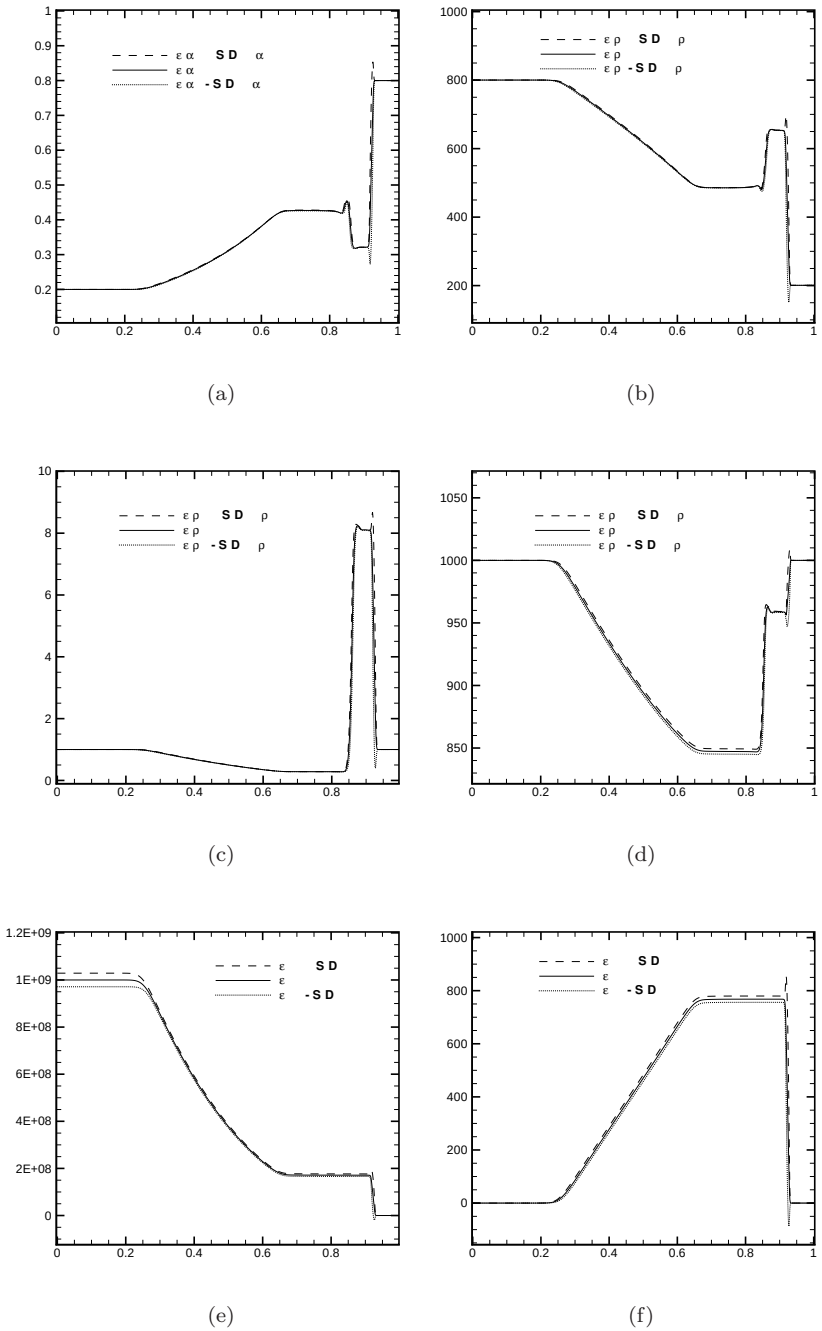

Figure 16: Confidence intervals ($\mu \pm \sigma$) for (a) gas volume fraction, (b) mixture density, (c) gas density, (d) liquid density, (e) mixture pressure and (f) mixture velocity. aSI scheme obtained with a level of 512 (m=9).

References

[1] A. Murrone and H. Guillard. A five equation reduced model for compressible two-phase flow problems. *Journal of Computational Physics*, 202:664–698, 2005.

[2] R. Abgrall. How to prevent pressure oscillations in multicomponent flow calculations: a quasi conservative approach. *Journal of Computational Physics*, 125:150–160, 1996.

[3] J. Massoni, R. Saurel, B. Nkonga, and R. Abgrall. Proposition de méthodes et modèles eulériens pour les problèmes à interfaces entre fluides compressibles en présence de transfert de chaleur: Some models and eulerian methods for interface problems between compressible fluids with heat transfer. *International Journal of Heat and Mass Transfert*, 45:1287–1307, 2002.

[4] A. Ambroso, C. Chalons, and P.-A. Raviart. A godunov-type method for the seven-equation model of compressible two-phase flow. *Computers and Fluids*, 54:67–91, 2012.

[5] R. Abgrall and V. Perrier. Asymptotic expansion of multiscale numerical scheme for compressible multiscale flow. *Society for Industrial and Applied Mathematics*, 5:84–115, 2006.

[6] E. Goncalves. Numerical study of expansion tube problems: Toward the simulation of cavitation. *Computers and Fluids*, 72:1–19, 2013.

[7] R. Saurel, F. Petitpas, and R. A. Berry. Simple and efficient relaxation methods for interfaces separating compressible fluids, cavitating flows and shocks in multiphase mixtures. *Journal of Computational Physics*, 228:16781712, 2009.

[8] A. K. Kapila, R. Menikoff, J. B. Bdzil, S. F. Son, and D. S. Stewart. Two-phase modeling of deflagration-to-detonation transition in granular materials: Reduced equations. *Physics of Fluids*, 13:3002–3024, 2001.

[9] M.R. Baer and J.W. Nunziato. A two-phase mixture theory for deflagration to detonation transition (ddt) in reactive granular materials. *International Journal of Multhiphase Flow*, 12:861–889, 1986.

[10] R. Saurel and R. Abgrall. A multiphase godunov method for compressible multifluid and multiphase flows. *Journal of Computational Physics*, 150:425–467, 1999.

[11] R. Saurel and O. Lemetayer. A multiphase model for compressible flows with interfaces, shocks,detonation waves and cavitation. *Journal of Fluid Mechanics*, 431:239–271, 2001.

[12] Y. Sun and C. Beckermann. Diffuse interface modeling of two-phase based on averaging:mass and momentum equations. *Physica D: Nonlinear Phenomena*, 198:281–308, 2004.

[13] O. Le Métayer, J. Massoni, and R. Saurel. Modelling evaporation fronts with reactive riemann solvers. *Journal of Computational Physics*, 205:567610, 2005.

[14] R. Abgrall and R. Saurel. Discrete equations for physical and numerical compressible multiphase mixtures. *Journal of Computational Physics*, 186:361–396, 2003.

[15] G. Allaire, S. Clerc, and S. Kokh. A five-equation model for the simulation of interfaces between compressible fluids. *Journal of Computational Physics*, 181:577–616, 2002.

[16] G.Perigaud and R. Saurel. A compressible flow model with capillary effects. *Journal of Computational Physics*, 209:139–178, 2005.

[17] R. Abgrall and M.G. Rodio. Discrete Equation Method (DEM) for the Simulation of Viscous, Compressible, Two-phase Flows. *Computers and Fluids*. doi: http://dx.doi.org/10.1016/j.compfluid.2013.11.028.

[18] I.G. Graham, F.Y. Kuo, D. Nuyens, R. Scheichl, and I.H. Sloan. Quasi-Monte Carlo methods for elliptic PDEs with random coefficients and applications. *Journal of Computational Physics*, 230(10):3668–3694, February 2011.

[19] Ivo Babuška, Fabio Nobile, and Raul Tempone. A Stochastic Collocation Method for Elliptic Partial Differential Equations with Random Input Data. *SIAM Review*, 52(2):317, 2010.

[20] Jasmine Foo and George Em Karniadakis. Multi-element probabilistic collocation method in high dimensions. *Journal of Computational Physics*, 229:1536–1557, March 2010.

[21] Olivier Le Maître. Uncertainty propagation using WienerHaar expansions. *Journal of Computational Physics*, 197(1):28–57, June 2004.

[22] Olivier Le Maître. Multi-resolution analysis of Wiener-type uncertainty propagation schemes. *Journal of Computational Physics*, 197(2):502–531, July 2004.

[23] J Tryoen, Olivier Le Maître, M Ndjinga, and A Ern. Intrusive Galerkin methods with upwinding for uncertain nonlinear hyperbolic systems. *Journal of Computational Physics*, 229:6485–6511, 2010.

[24] Julie Tryoen. *Methodes de Galerkin stochastiques adaptatives pour la propagation d'incertitudes parametriques dans les systemes hyperboliques*. PhD thesis, Univeriste Paris-Est.

[25] P Pettersson and Gianluca Iaccarino. Numerical analysis of the Burgers equation in the presence of uncertainty. *Journal of Computational Physics*, 228:8394–8412, 2009.

[26] R. Abgrall and P.M. Congedo. A semi-intrusive deterministic approach to uncertainty quantification in non-linear fluid flow problems. *Journal of Computational Physics*, 235:828–845, 2013.

[27] R. Abgrall, P.M. Congedo, G. Geraci, and G. Iaccarino. An adaptive multiresolution semi-intrusive scheme for uq in compressible fluid problems. *International Journal for Numerical Methods in Fluids*. Submitted.

[28] A. Gel, R. Garg, C. Tong, M. Shahnam, and C. Guenther. Applying uncertainty quantification to multiphase flow computational fluid dynamics. *Powder Technology*, 242:27–39, 2013.

[29] K. K. So, T. Chantrasmi, X.Y. Hu, J. Witteveen, C. Stemmer, G. Iaccarino, and et al. Uncertainty analysis for shock-bubble interaction. In *Proceedings of the 2010 summer program, center for turbulence research. USA: Stanford University.*, 2010.

[30] M. Presho, A. Malqvist, and V. Ginting. Density estimation of two-phase flow with multiscale and randomly perturbed data. *Advances in Water Resources*, 33:1130–1141, 2010.

[31] R. Conejeros and B. Lenoach. Effect of uncertainty on 2-phase flow into a horizontal completion. *Journal of Petroleum Science and Engineering*, 58:309–324, 2007.

[32] H. Li and D. Zhang. Efficient and accurate quantification of uncertainty for multiphase flow with the probabilistic collocation method. *SPE J.*, 14:665–679, 2009.

[33] M.G. Rodio and P.M. Congedo. Robust analysis of cavitating flows in the Venturi tube. *European Journal of Mechanics - B/Fluids*, 44:88–99, 2014. doi:http://dx.doi.org/10.1016/j.euromechflu.2013.11.002.

[34] P. Pettersson, G. Iaccarino, and J. Nordstrom. An intrusive hybrid method for discontinuous two-phase flow under uncertainty. *Computers and Fluids*, 86:228–239, 2013.

[35] Rémi Abgrall, Pietro Marco Congedo, and Gianluca Geraci. A One-Time Truncate and Encode Multiresolution Stochastic Framework. *Journal of Computational Physics*, 257:19–56, 2014. http://dx.doi.org/10.1016/j.jcp.2013.08.006.

[36] Rémi Abgrall, Pietro Marco Congedo, and Gianluca Geraci. Towards a Unified Multiresolution Scheme in the Combined Physical / Stochastic Space for Stochastic Differential Equations. *Mathematics and Computers in Simulation*, 2012. Submitted.

[37] Technical report.

[38] D.A. Drew and S.L. Passman. *Theory of Multicomponent Fluids*, volume 135. Applied Mathematical Sciences, Springer, New York, 1998.

[39] F. Coquel and B. Perthame. Relaxation of energy and approximate riemann solvers for general pressure laws in fluid dynamics. *Society for Industrial and Applied Mathematics*, 35:2223–2249, 1998.

[40] E.F. Toro. *Riemann Solvers and Numerical Methods for Fluid Dynamics.* Springer, Berlin, 1997.

[41] Ami Harten. Adaptive multiresolution schemes for shock computations. *Journal of Computational Physics*, 115(2):319–338, August 1994.

[42] Ami Harten. Multiresolution algorithms for the numerical solution of hyperbolic conservation laws. *Communications on Pure and Applied Mathematics*, 48(12):1305–1342, 1995.

[43] Ami Harten. Multiresolution Representation of Data : A General Framework. *SIAM Journal on Numerical Analysis*, 33(3):1205–1256, 1996.

[44] Rémi Abgrall, Pietro Marco Congedo, Gianluca Geraci, and Gianluca Iaccarino. Non-linear Multiresolution framework for Uncertainty Quantification in Computational Fluid Dynamics. *Journal of Computational and Applied Mathematics*, 2013. Submitted.

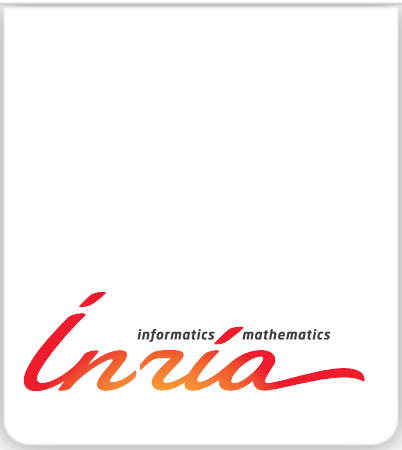

RESEARCH CENTRE
BORDEAUX – SUD-OUEST

351, Cours de la Libération
Bâtiment A 29
33405 Talence Cedex

Publisher
Inria
Domaine de Voluceau - Rocquencourt
BP 105 - 78153 Le Chesnay Cedex
inria.fr

ISSN 0249-6399